BEST AVAILABLE IMAGES

Defective images within this document are accurate representations of the original documents submitted by the applicant.

Defects in the images may include (but are not limited to):

- BLACK BORDERS
- TEXT CUT OFF AT TOP, BOTTOM OR SIDES
- FADED TEXT
- ILLEGIBLE TEXT
- SKEWED/SLANTED IMAGES
- COLORED PHOTOS
- BLACK OR VERY BLACK AND WHITE DARK PHOTOS
- GRAY SCALE DOCUMENTS

IMAGES ARE BEST AVAILABLE COPY.

As rescanning documents *will not* correct images, please do not report the images to the Image Problem Mailbox.

)T Vol. 7, No. 15 August 2002

Macroresults through Microarrays

John C. Rockett, Reproductive Toxicology Division (MD-72), National Health and Environmental Effects Research Laboratory, Office of Research and Development, US Environmental Protection Agency, Research Triangle Park, 2525 East Highway 54, Durham, NC 27711, USA; tel: +1 919 541 2071, fax: +1 919 541 4017, e-mail: rockett.john@epa.gov

The third enactment of Cambridge Healthtech Institute's *Macroresults through Microarrays* meeting was held in Boston (MA, USA) from 29 April–1 May 2002. The subtheme of this year's meeting was 'advancing drug discovery', a widely touted application for array technology.

The evolution of microarrays

If you were asked 'Who first conceived of the idea of microarrays', who would come to mind? Mark Schena perhaps, first author of the seminal 1995 paper on cDNA arrays [1]? Maybe Pat Brown, Schena's then supervisor? Or perhaps Stephen Fodor, the primary driver behind Affymetrix's (http://www.affymetrix.com) oligonucleotide-based platform [2]. Brits might even chant the name of Ed Southern [3]. Well, according to Roger Ekins (University College London Medical School; http://www.ucl.ac.uk/medicine/) all these answers would be wrong. It was in fact Ekins and his colleagues who first conceived of and patented 'a new generation of ultrasensitive, miniaturized assays for protein and DNA–RNA measurement based on the use of microarrays' in the mid 1980s [4]. The concept and potential of array technology was more fully described in a later publication, in which Ekins *et al.* [5] concluded that antibody microspots of ~50 μm^2 could be achieved, and that as many as 2 million different immunoassays could, in principle, be accommodated on a surface area of 1 cm^2.

Technological innovation

In practice, it took a different biological molecule (DNA), a different research group, and a leap into microfabrication technology to even begin approaching these kinds of densities [Affymetrix patent 6045996 talks of one million spots cm^{-2}]. Of course, advancing technology is one of the driving engines behind the genomics juggernaut, and we are already seeing '4th generation' machines for fabricating DNA chips. If the company representatives at this meeting are to be believed (and their cases seemed strong), spotting is out, and *in situ* fabrication of oligonucleotide-based 'iterative custom arrays' is in. Whether you go with the Combimatrix's (http://www.combimatrix.com) electrochemically directed synthesis and detection system, febit's (http://www.febit.com) Geniom® technology, or Nimblegen's (http://www.nimblegen.com) Maskless Array Synthesizer technology is a matter of personal choice. However, each of these machines provides the flexibility to design variable length oligonucleotide probes from sequences inputted by the user, and then perform *in situ* synthesis of an array. Each system also boasts unique advantages. For example, Combimatrix's biological array processor is a semiconductor coated with a 3D layer of porous material in which DNA, RNA, peptides or small molecules can be synthesized or immobilized within discrete test sites, while febit's Geniom One® is a fully integrated gene-expression analysis system with minimal user hands-on time – the probe sequences are programmed, the RNA samples inserted, and the gene expression data is pumped out a few hours later.

Cell- and tissue-based arrays

Array technology is in most people's minds firmly linked with gene-expression profiling. Fewer are aware that cell- and tissue-based arrays have been developed, and how they can provide a vital extra dimension to research. In support of this, Barry Bochner gave an update on the cell-based array system that Biolog (http://www.biolog.com) has produced for simultaneously measuring the effects of one gene in the cell under thousands of growth conditions (see [6] for further details). David Walt (Tufts University; http://www.tufts.edu/) is developing single live cell arrays using optical imaging fiber (OIF) technology. An array of microwells is fabricated on the face of an OIF at densities of up to 10 million wells cm^{-2}. Cells are then added to the wells and disperse at an average of one cell per well. Physiological and genetic responses of each cell are measured via fluorescence produced by reporter genes (e.g. *lacZ*, *gfp*. Assays performed so far include yeast live or dead cell assay, microenvironment pH and O_2 measurements, promotor responses using the *lacZ* and *phoA* reporter genes, and protein–protein interactions using the yeast two-hybrid system. The main advantage of this system is that the cells remain alive during the assay, which means a real-time timecourse can be performed and/or the array passed from sample to sample. This would be useful in, for example, the scanning of a combinatorial drug library for specific physiological effects.

Tissue arrays are a useful complementary technology to DNA arrays because they can be used to help validate and

understand the biological and medical significance of gene changes discovered using standard DNA arrays. For example, an array of tumor tissues can be screened for the protein (using immunohistochemistry), message (using *in situ* hybridization) and copy number (using comparative genomic hybridization) of a gene of interest, to determine if expression of the gene (or lack thereof) is related in any way to survival. They can also be used to predict the probability of clinical failure of lead compounds as a result of toxicity by evaluating the distribution of the drug targets in normal tissue. Spyro Mousses and his co-workers at the National Human Genome Research Institute (http://www.nhgri.nih.gov/index.html) have built such arrays, including a multi-tumor array (~5000 specimens, and sections from 36 normal and 800 metastatic tissues) and a normal tissue array (76 tissue and 332 cell types).

The problem with proteins

It has been said that genomics tells us what might happen, transcriptomics indicates what should happen, and proteomics shows what is happening. The impact of functional proteomics on pharmaceutical R&D is rapidly increasing, and protein arrays are being used increasingly in both basic and applied research. Their use lies not only in comparative protein expression and interaction profiling, but also in diagnostics and drug discovery. However, an increasing number of researchers have found that protein arrays, like their cousins the DNA arrays, present several practical obstacles relating to their production and use. For example, in using *Escherichia coli* to produce recombinant eukaryotic proteins from a single expression vector, multiple protein products are often produced, suggesting mixes of truncated or otherwise altered proteins. There is also the obvious concern that the proteins might not be modified in a similar manner to eukaryotic systems. Also, an optimal method for depositing and binding proteins to the selected substrate is yet to be determined, as is the best way to ensure that they are bound in a correctly folded, active conformation.

Several companies have been addressing these problems. Prolinx (http://www.prolinxinc.com) is one such company, and Karin Hughes described their Versalinx™ chemistry for producing protein, peptide and small-molecule arrays. Versalinx™ uses solution-phase conjugation followed by immobilization, resulting in functional orientation of proteins and peptides on the substrate surface. It also offers the valuable additional benefit of exhibiting low non-specific binding. Sense Proteomic (http://www.senseproteomic.com) is also among those addressing these problems to develop robust protein arrays for drug discovery and clinical applications and has developed functional protein array formats based on specific disease tissues. Subtractive hybridization is used to identify genes with altered expression in breast tumor and cystic fibrosis compared to normal tissue. A high throughput cloning strategy (COVET™) is then used to produce libraries of genes that are tagged, cloned, expressed, purified and finally immobilized on glass slides. Initial validation studies have shown that the vast majority of the immobilized proteins do indeed retain biological function.

Stefan Schmidt and his company (GPC Biotech; http://www.gpcbiotech.de) have moved past the platform development stage and, with their focus firmly on drug discovery, are currently developing kinase-profiling arrays. Kinases are important targets for pharmaceutical drug discovery and therapy, and GPC's aim is to simultaneously detect multiple kinases, obtain activity profiles for different cell types, or analyze the ability of drug candidates to inhibit kinase activity. To do this, recombinant kinase substrates are immobilized on membranes, incubated with purified kinase, and the substrates measured for the degree of phosphorylation.

Summary

Meetings like this, packed with exciting discoveries and intriguing and interesting innovation, heavily emphasize the pace at which biotechnology is advancing, to the extent that the number of options for genomic and proteomic researchers can become overwhelming. Although data analysis is perhaps the greatest current concern for array users, an increasing challenge will be to determine the approaches and technology that really work, and to do it in a timely manner.

References

1 Schena, M. *et al.* (1995) Quantitative monitoring of gene expression patterns with a complementary DNA microarray. *Science* 270, 467–470
2 Fodor, S.P. *et al.* (1991) Light-directed, spatially addressable parallel chemical synthesis. *Science* 251, 767–773
3 Southern, E.M. *et al.* (1992) Analyzing and comparing nucleic acid sequences by hybridization to arrays of oligonucleotides: evaluation using experimental models. *Genomics* 13, 1008–1017
4 Ekins, R.P. (1987) US Patent Application 8 803 000
5 Ekins, R. *et al.* (1989) High specific activity chemiluminescent and fluorescent markers: their potential application to high sensitivity and 'multi-analyte' immunoassays. *J. Biolum. Chemilum.* 4, 59–78
6 Rockett, J.C. (2002) Chip, chip, array! Three chips for post-genomic research. *Drug Discov. Today* 7, 458–459

Acknowledgements

I would like to thank Mary Ann Brown (Cambridge Healthtech Institute) and David Dix (US EPA) for critical review of this manuscript prior to submission. This document has been reviewed in accordance with US Environmental Protection Agency policy and approved for publication. Mention of companies, trade names or products does not signify endorsement of such by the EPA.

Electrophoresis 1991, *12*, 907–930

N. Leigh Anderson
Ricardo Esquer-Blasco
Jean-Paul Hofmann
Norman G. Anderson

Large Scale Biology Corporation, Rockville, MD

A two-dimensional gel database of rat liver proteins useful in gene regulation and drug effects studies

A standard two-dimensional (2-D) protein map of Fischer 344 rat liver (F344MST3) is presented, with a tabular listing of more than 1200 protein species. Sodium dodecyl sulfate (SDS) molecular mass and isoelectric point have been established, based on positions of numerous internal standards. This map has been used to connect and compare hundreds of 2-D gels of rat liver samples from a variety of studies, and forms the nucleus of an expanding database describing rat liver proteins and their regulation by various drugs and toxic agents. An example of such a study, involving regulation of cholesterol synthesis by cholesterol-lowering drugs and a high-cholesterol diet, is presented. Since the map has been obtained with a widely used and highly reproducible 2-D gel system (the Iso-Dalt® system), it can be directly related to an expanding body of work in other laboratories.

Contents

1 Introduction

High-resolution two-dimensional electrophoresis of proteins, introduced in 1975 by O'Farrell and others [1–4], has been used over the ensuing 16 years to examine a wide variety of biological systems, the results appearing in more than 5000 published papers. With the advent of computerized systems for analyzing two-dimensional (2-D) gel images and constructing spot databases, it is also possible to plan and assemble integrated bodies of information describing the appearance and regulation of thousands of protein gene products [5, 6]. Creating such databases involves amassing and organizing quantitative data from thousands of 2-D gels, and requires a substantial commitment in technology and resources.

Given the long-term effort required to develop a protein database, the choice of a biological system takes on considerable importance. While *in vitro* systems are ideal for answering many experimental questions, especially in cancer research and genetics, our experience with cell cultures and tissue samples suggests that some *in vivo* approaches could have major advantages. In particular, we have noticed that liver tissue samples from rats and mice appear to show greater quantitative reproducibility (in terms of individual protein expression) than replicate cell cultures. This is perhaps a natural result of the homeostasis maintained in a complete animal *vs.* the well-known variability of cell cultures, the latter due principally to differences in reagents (*e.g.*, fetal bovine serum), conditions (*e.g.*, pH) and genetic "evolution" of cell lines while in culture. It is also more difficult to generate adequate amounts of protein from cell culture systems (particularly with attached cells), forcing the investigator to resort to radioisotope-based or silver-based stain-detection methods. While these methods are more sensitive (sometimes much more sensitive) than the Coomassie Brilliant Blue (CBB) stain typically used for protein detection in "large" protein samples, they are generally more variable, more labor-intensive and, in the case of radiographic methods, may generate highly "noisy" images, due to the properties of the films used. By contrast, large protein samples can easily be prepared from liver using urea/Nonidet P-40 (NP-40) solubilization and stained with CBB, which has the advantage of being easily reproducible [8]. Finally, there remains the question of the "truthfulness" of many *in vitro* systems as compared to their *in vivo* analogs; how great are the changes caused by the introduction into a cul-

Correspondence: Dr. N. Leigh Anderson, Large Scale Biology Corporation, 9620 Medical Center Drive, Rockville, MD 20850, USA

Abbreviations: CBB, Coomassie Brilliant Blue; CPK, creatine phosphokinase; 2-D, two-dimensional; IEF, isoelectric focusing; MSN, master spot number; NP-40, Nonidet P-40, SDS, sodium dodecyl sulfate

0173-0835/91/1111-0907 $3.50+.25/0

ture and the associated shift to strong selection for growth, and how do these affect experimental outcomes? Hence the apparent advantages of *in vitro* systems, in terms of experimental manipulation, may be counterbalanced by other factors relating to 2-D data quality.

There is a second important class of reasons for exploring the use of an *in vivo* biological system such as the liver. Historically, there have been two broad approaches to the mechanistic dissection of biochemical processes in intact cellular systems: genetics (a search for informative mutants) and the use of chemical agents (drugs and chemical toxins). Both approaches help us to understand complex systems by disrupting some specific functional element and showing us the result. With the development of techniques for genetic manipulation and cloning, the genetic approach can be effectively applied either *in vitro* or *in vivo*, although the *in vitro* route is usually quicker. The chemical approach can also be applied to either sort of biological system; here, however, the bulk of consistently acquired information is in experimental animals (rats and mice). While most biologists know a short list of compounds having specific, experimentally useful effects (*e.g.*, inhibitors of protein synthesis, ionophores, polymerase inhibitors, channel blockers, nucleotide analogs, and compounds affecting polymerization of cytoskeletal proteins), there is a much larger number of interesting chemically-induced effects, most of them characterized by toxicologists and pharmacologists in rodent systems. Just as a thorough genetic analysis would involve saturating a genome with mutations, it is possible to imagine a saturating number of drugs, the analysis of whose actions would reveal the complete biochemistry of the cell. While organized drug discovery efforts usually target specific desired effects, the nature of the process, with its dependence on screening large numbers of compounds, necessarily produces many unanticipated effects. It is therefore reasonable to suppose that the required broad range of compounds necessary to achieve "biochemical saturation" may be forthcoming; in fact, it may already exist among the hundreds of thousands of compounds that failed to qualify as drugs.

Among organs, the liver is an obvious choice for the study of chemical effects because of its well-known plasticity and responsiveness. The brain appears to be quite plastic (*e.g.* [7]), but it is a complicated mixture of cell types requiring skillful dissection for most experiments. The kidney, while quite responsive, also presents a potentially confounding mixture of cell types. The liver, by contrast, is made up of one predominant cell type which is easy to solubilize: the hepatocyte, representing more than 95% of its mass. Most importantly, the liver performs many homeostatic functions that require rapid modulation of gene expression. It appears that most chemical agents tested affect gene expression in the liver at some dosage (N. Leigh Anderson, unpublished observations), an interesting contrast to our earlier work with lymphocytes, for example, which seem to be much less responsive. Such results conform to the expectation that cells with a homeostatic, physiological role should be more plastic than cells differentiated for a purpose dependent on the action of a limited number of specific genes.

The liver also allows the parallels between *in vitro* and *in vivo* systems to be examined in detail. Significant progress has been made in the development of mouse, rat and human hepatocyte culture systems, as well as in precision-cut tissue slices. Using such an array of techniques, it is possible to assemble a matrix of mammalian systems including mouse and rat *in vivo* on one level and mouse, rat and human *in vitro* on a second level, and to compare effects between species and between systems. This approach allows us to draw informed conclusions regarding the biochemical "universality" of biological responses among the mammals, and to offer some insight into the validity of *in vitro* approaches for toxicological screening. We believe this data will be necessary if *in vitro* alternatives are to achieve wide usage in government-mandated safety testing of drugs, consumer products and industrial and agricultural chemicals.

A number of interesting studies have been published using 2-D mapping to examine effects in the rodent liver. A number of investigarors have made use of the technique to screen for existing genetic variants [8–11] or induced mutations [12–14], mainly in the mouse. This work builds on the wealth of genetic information available on the mouse and its established position as a mammalian mutation-detection system. While some studies of chemical effects have been undertaken in the mouse [15–17], most have used the rat [18–23]. The examination of the cytochrome p-450 system, in particular, has been carried out almost exclusively on the rat [24, 25].

These considerations lead us to conclude that rodent liver offers the best opportunity to systematically examine an array of gene regulation systems, and ultimately to build a predictive model of large-scale mammalian gene control. The basic underlying foundation of such a project is a reliable, reproducible master 2-D pattern of liver, to which ongoing experimental results can be referred. In this paper, we report such a master pattern for the acidic and neutral proteins of rat liver (pattern F344MST3). In future, this master will be supplemented by maps of basic proteins, and analogous maps of mouse and human liver.

2 Materials and methods

2.1 Sample preparation

Liver is an ideal sample material for most biochemical studies, including 2-D analysis. A sample is taken of approximately 0.5 g of tissue from the apical end of the left lobe of the liver. Solubilization is effected as rapidly as practical; a delay of 5–15 min appears to cause no major alteration in liver protein composition if the liver pieces are kept cold (*e.g.*, on ice) in the interim. In the solubilization process, the liver sample is weighed, placed in a glass homogenizer (*e.g.*, 15 mL Wheaton); 8 volumes of solubilizing solution*

* The solubilizing solution is composed of 2% NP-40 (Sigma), 9 M urea (analytical grade, *e.g.*, BDH or Bio-Rad), 0.5% dithiothreitol (DTT; Sigma) and 2% carrier ampholytes (pH 9–11 LKB: these come as a 20% stock solution, so 2% final concentration is achieved by making the final solution 10% 9–11 Ampholine by volume). A large batch of solubilizer (several hundred mL) is made and stored frozen at –80 °C in aliquots sufficient to provide enough for one day's estimated sample preparation requirement. The solution is never allowed to become warmer than room temperature at any stage during preparation or thawing for use, since heating of concentrated urea solutions can produce contaminants that covalently modify proteins producing artifactual charge shifts. Once thawed, any unused solubilizer is discarded.

is added (*i.e.*, 4 mL per 0.5 g tissue) and the mixture is homogenized using first the loose- and then then the tight-fitting glass pestle. This takes approximately 5 strokes with each pestle and is carried out at room temperature because urea would crystallize out in the cold. Once the liver sample is thoroughly homogenized in the solubilizer, it is assumed that all the proteins are denatured (by the chaotropic effect of the urea and NP-40 detergent) and the enzymes inactivated by the high pH (~9.5). Therefore these samples may be kept at room temperature until they can be centrifuged or frozen as a group (within several hours of preparation). The samples are centrifuged for 6×10^6 *g* min (*e.g.*, 500 000 × *g* for 12 min using a Beckman TL-100 centrifuge). The centrifuge rotor is maintained at just below room temperature (*e.g.*, 15–20°C), but not too cold, so as to prevent the precipitation of urea. The centrifuge of choice is a Beckman TL-100 because of the sample tube sizes available, but any ultracentrifuge accepting smallish tubes will suffice. When an appropriate centrifuge is not available near the site of sample preparation, samples can be frozen at −80°C and thawed prior to centrifugation and collection of supernatants. Each supernatant is carefully removed following centrifugation and aliquoted into at least 4 clean tubes for storage. This is done by transferring all the supernatant to one clean tube, mixing this gently (to assure homogeneous composition) and then dividing it into 4 aliquots. The aliquots are frozen immediately at −80°C. These multiple aliquots can provide insurance against a failed run or a freezer breakdown.

2.2 Two-dimensional electrophoresis

Sample proteins are resolved by 2-D electrophoresis using the 20 × 25 cm Iso-Dalt® 2-D gel system ([26–29]; produced by LSB and by Hoefer Scientific Instruments, San Francisco) operating with 20 gels per batch. All first-dimensional isoelectric focusing (IEF) gels are prepared using the same single standardized batch of carrier ampholytes (BDH 4–8A in the present case, selected by LSB's batch-testing program for rat and mouse database work**). A 10 µL sample of solubilized liver protein is applied to each gel, and the gels are run for 33 000 to 34 500 volt-hours using a progressively increasing voltage protocol implemented by a programmable high-voltage power supply. An Angelique™ computer-controlled gradient-casting system (produced by LSB) is used to prepare second-dimensional sodium dodecyl sulfate (SDS) polyacrylamide gradient slab gels in which the top 5% of the gel is 11%T acrylamide, and the lower 95% of the gel varies linearly from 11% to 18%T.

This system has recently been modified so as to employ a commercially available 30.8%T acrylamide/*N,N'*-methylenebisacrylamide prepared solution (thus avoiding the handling of the solid acrylamide monomer) and three additional stock solutions: buffer (made from Sigma pre-set Tris), persulfate and *N,N,N',N'*-tetramethylethylenediamine (TEMED). Each gel is identified by a computer-printed filter paper label polymerized into the lower left corner of the gel. First-dimensional IEF tube gels are loaded directly (as extruded) onto the slab gels without equilibration, and held in place by polyester fabric wedges (Wedgies™, produced by LSB) to avoid the use of hot agarose. Second-dimensional slab gels are run overnight, in groups of 20, in cooled DALT tanks (10°C) with buffer circulation. All run parameters, reagent source and lot information, and notations of deviation from expected results are entered by the technician responsible on a detailed, multi-page record of the experiment.

2.3 Staining

Following SDS-electrophoresis, slab gels are stained for protein using a colloidal Coomassie Blue G-250 procedure in covered plastic boxes, with 10 gels (totalling approximately 1 L of gel) per box. This procedure (based on the work of Neuhoff [30, 31]) involves fixation in 1.5 L of 50% ethanol and 2% phosphoric acid for 2 h, three 30 min washes, each in 2 L of cold tap water, and transfer to 1.5 L of 34% methanol, 17% ammonium sulfate and 2% phosphoric acid for 1 h, followed by the addition of a gram of powdered Coomassie Blue G-250 stain. Staining requires approximately 4 days to reach equilibrium intensity, whereupon gels are transferred to cool tap water and their surfaces rinsed to remove any particulate stain prior to scanning. Gels may be kept for several months in water with added sodium azide. The water washes remove ethanol that would dissolve the stain (and render the system noncolloidal, with high backgrounds). The concentrated ammonium sulfate and methanol solution is diluted by equilibration with the water volume of the gels to automatically achieve the correct final concentrations for colloidal staining. Practical advantages of this staining approach can be summarized as follows: (i) the low, flat background makes computer evaluation of small spots (max OD < 0.02) possible, especially when using laser densitometry; (ii) up to 1500 spots can be reliably detected on many gels (*e.g.*, rat liver) at loadings low enough to preserve excellent resolution; and (iii) reproducibility appears to be very good: at least several hundred spots have coefficients of reproducibility less than 15%. This value is at least as good as previous CBB methods, and significantly better than many silver stain systems.

2.4 Positional standardization

The carbamylated rabbit muscle creatine phosphokinase (CPK) standards [32] are purchased from Pharmacia and BDH. Amino acid compositions, and numbers of residues present in proteins used for internal standardization, are taken from the Protein Identification Resource (PIR) sequence database [33].

2.5 Computer analysis

Stained slab gels are digitized in red light at 134 micron resolution, using either a Molecular Dynamics laser scanner (with pixel sampling) or an Eikonix 78/99 CCD scanner. Raw digitized gel images are archived on high-density DAT tape (or equivalent storage media) and a greyscale videoprint prepared from the raw digital image as hard-copy backup of the gel image. Gels are processed using the Kepler® software system (produced by LSB), a commercially available workstation-based software package built on

** This material (succeeding certified batches of which are available from Hoefer Scientific Instruments) has the most linear pH gradient produced by any ampholyte tested except for the Pharmacia wide range (which has an unacceptable tendency to bind high-molecular weight acidic proteins, causing them to streak).

some of the principles of the earlier TYCHO system [34–41]. Procedure PROC008 is used to yield a spotlist giving position, shape and density information for each detected spot. This procedure makes use of digital filtering, mathematical morphology techniques and digital masking to remove the background, and uses full 2-D least-squares optimization to refine the parameters of a 2-D Gaussian shape for each spot. Processing parameters and file locations are stored in a relational database, while various log files detailing operation of the automatic analysis software are archived with the reduced data. The computed resolution and level of Gaussian convergence of each gel are inspected and archived for quality control purposes.

Experiment packages are constructed using the Kepler experiment definition database to assemble groups of 2-D patterns corresponding to the experimental groups (*e.g.*, treated and control animals). Each 2-D pattern is matched to the appropriate "master" 2-D pattern (pattern F344MST3 in the case of Fischer 344 rat liver), thereby providing linkage to the existing rodent protein 2-D databases. The software allows experiments containing hundreds of gels to be constructed and analyzed as a unit, with up to 100 gels displayed on the screen at one time for comparative purposes and multiple pages to accommodate experiments of $>$ 1000 gels. For each treatment, proteins showing significant quantitative differences *vs.* appropriate controls are selected using group-wise statistical parameters (*e.g.*, Student's t-test, Kepler® procedure STUDENT). Proteins satisfying various quantitative criteria (such as $P <$ 0.001 difference from appropriate controls) are represented as highlighted spots onscreen or on computer-plotted protein maps and stored as spot populations (*i.e.*, logical vectors) in a liver protein database. Quantitative data (spot parameters, statistical or other computed values) are stored as real-valued vectors in the database. Analysis of coregulation is performed using a Pierson product-moment correlation (Kepler procedure CORREL) to determine whether groups of proteins are coordinately regulated by any of the treatments. Such groups can be presented graphically on a protein map, and reported together with the statistical criteria used to assess the level of coregulation. Multivariate statistical analysis (*e.g.*, principal components' analysis) is performed on data exported to SAS (SAS Institute).

2.6 Graphical data output

Graphical results are prepared in GKS and translated within Kepler® into output for any of a variety of devices. Linedrawing output is typically prepared as Postscript and printed on an Apple Laserwriter. Detailed maps presented here have been generated using an ultra-high-resolution Postscript-compatible Linotronic output device. Greyscale graphics are reproduced from the workstation screen using a Seikosha videoprinter. Patterns are shown in the standard orientation, with high molecular mass at the top and acidic proteins to the left.

2.7 Experiment LSBC04

In the study described here 12-week-old Charles River male F344 rats were used. Diets were prepared at LSB, based on a Purina 5755M Basal Purified Diet. Lovastatin and cholestyramine were obtained as prescription pharmaceuticals, ground and mixed with the diet at concentrations of 0.075% and 1%, respectively. The high cholesterol diet was Purina 5801M-A (5% cholesterol plus 1% sodium cholate in the control diet). Animal work was carried out by Microbiological Associates (Bethesda, MD). Animals were acclimatized for one week on the control diet, fed test or control diets for one week, and sacrificed on day 8. Average daily doses of lovastatin and cholestyramine in appropriate groups were 37 mg/kg/day and 5 g/kg/day, respectively, based on the weight of the food consumed. Liver samples were collected and prepared for 2-D electrophoresis according to the standard liver protocol (homogenization in 8 volumes of 9 M urea, 2% NP-40, 0.5% dithiothreitol, 2% LKB pH 9–11 carrier ampholytes, followed by centrifugation for 30 min at 80000 $\times$ *g*). Kidney, brain and plasma samples were frozen. Gels were run as described above, and the data was analyzed using the Kepler® system. Gels were scaled, to remove the effect of differences in protein loading, by setting the summed abundances of a large number of matched spots equal for each gel (linear scaling).

3 Results and discussion

3.1 The rat liver protein 2-D map

F344MST3 is a standard 2-D pattern of rat liver proteins, based on the Fischer 344 strain. This pattern was initiated from a single 2-D gel and extensively edited in an experiment comparing it to a range of protein loads, so as to include both small spots and well-resolved representations of high-abundance spots. More than 700 rat liver 2-D patterns have been matched to F344MST3 in a series of drug effects and protein characterization experiments, and numerous new spots (induced by specific drugs, for instance) have been added as a result. A modified version including additional spots present in the Sprague-Dawley outbred rat has also been developed (data not shown). Figure 1 shows a greyscale representation and Fig. 2 a schematic plot of the master pattern. More than 1200 spots are included, most of which are visible on typical gels loaded with 10 µL of solubilized liver protein prepared by the standard method and stained with colloidal Coomassie Blue. Master spot numbers (MSN's) have been assigned to all proteins, and appear in the following figures, each showing one quadrant of the pattern. Figure 3 shows the upper left (acidic, high molecular mass) quadrant, Fig. 4 the upper right (basic, high molecular mass) quadrant, Fig. 5 the lower left (acidic, low molecular mass) quadrant, and Fig. 6 the lower right (basic, low molecular mass) quadrant. The quadrants overlap as an aid to moving between them. The gel position (in 100 micron units), isoelectric point (relative to the CPK internal p*I* standards) and SDS molecular mass (from the calibration curve in Fig. 8) are listed for each spot (Table 1). Because of the precision of the CPK-p*I* values, these parameters can be used to relate spot locations between gel systems more reliably than using p*I* measurements expressed as pH. A major objective of current studies is the identification of all major spots corresponding to known liver proteins, as well as rigorous definitions of subcellular organelle contents. Of particular interest to us is the parallel development of identifications in the rat and mouse liver maps, allowing detailed comparisons of gene expression effects in the two systems. The results of these studies will be presented systematically in a later edition of this database,

but we include here a useful series of 22 orienting identifications as an aid to other users of the rat liver pattern (Table 2).

3.2 Carbamylated charge standards, computed p*I*s and molecular mass standardization

We have previously shown that the use of a system of closely-spaced internal p*I* markers (made by carbamylating a basic protein) offers an accurate and workable solution to the problem of assigning positions in the p*I* dimension [32]. The same system, based on 36 protein species made by carbamylating rabbit muscle CPK, has been used here to assign p*I*s to most rat liver acidic and neutral proteins. The standards were coelectrophoresed with total liver proteins, and the standard spots added to a special version of the master pattern F344MST3. The gel *X*-coordinates of all liver protein spots lying within the CPK charge train were then transformed into CPK p*I* positions by interpolation between the positions of immediately adjacent standards (Table 1) using a Kepler® vector procedure.

It has proven possible to compute fairly accurate p*I* values for many proteins from the amino acid composition [42]. We have attempted here to test a further elaboration of this approach, in which we computed p*I*s for the CPK standards themselves, based on our knowledge of the rabbit muscle CPK sequence and the fact that adjacent members of the charge train typically differ by blockage of one additional lysine residue (Table 3). We compared these values to similar computed p*I*s for an additional set of carbamylated standards made from human hemoglobin beta chains and a series of rat liver and human plasma proteins of known position and sequence (Fig. 7, Table 4). The result demonstrates good concordance between these systems. Two proteins show significant deviations: liver fatty-acid binding protein (FABP; #1 in Table 4) and protein disulphide isomerase (#20 in the table). The FABP spot present on F344MST3 may represent a charge-modified version of a more basic parent spot closer to the expected p*I*, not resolved in the IEF/SDS gel. Of particular importance is the fact that, by comparing computed p*I*s of sequenced but unlocated proteins with the CPK p*I*s, we can assign a probable gel location without making any assumptions regarding the actual gel pH gradient. This offers a useful shortcut, given the vagaries of pH measurement on small diameter IEF gels. We have used this approach to compute the CPK p*I*s of all rat and mouse proteins in the PIR sequence database, as an aid to protein identification (data not shown).

In order to standardize SDS molecular weight (SDS-MW), we have used a standard curve fitted to a series of identified proteins (Fig. 8). Rather than using molecular mass *per se*, we have elected to use the number of amino acids in the polypeptide chain, as perhaps a better indication of the length of the SDS-coated rod that is sieved by the second dimension slab. The resulting values were multiplied by 112 (the weighted average mass of amino acids in sequenced proteins) to give predicted molecular masses. Because we use gradient slabs, we have not constrained the fitted curve to conform to any predetermined model; rather we tried many equations and selected the best using the program "Tablecurve" on a PC. The equation chosen was $y = a + bx + c/x^2$, where y is the number of residues, x is the gel *Y* coordinate, a is 511.83, b is −0.2731 and c is 33183801. The resulting fit appears to be fairly good over a broad range of molecular mass.

3.3 An example of rat liver gene regulation: Cholesterol metabolism

Experiment LSBC04 was designed as a small-scale test of the regulation of cholesterol metabolism *in vivo* by three agents included in the diet: lovastatin (Mevacor®, an inhibitor of HMG-CoA reductase); cholestyramine (a bile acid sequestrant that has the effect of removing cholesterol from the gut-liver recirculation); and cholesterol itself. The first two agents should lower available cholesterol and the third should raise it, allowing manipulation of relevant gene expression control systems in both directions. Such an experiment offers an interesting test of the 2-D mapping system since most of the pathway enzymes are present in low abundance, many are membrane-bound and difficult to solubilize, and the pathway itself is complex. Approximately 1000 proteins were separated and detected in liver homogenates. Twenty-one proteins were found to be affected by at least one treatment, and these could be divided into several coregulated groups.

3.3.1 MSN 413 (putative cytosolic HMG-CoA synthase) and sets of spots regulated coordinately or inversely

One group of spots (including a spot assigned to the cytosolic HMG-CoA synthase, MSN 413) showed the expected increase in abundance with lovastatin or cholestyramine, the synergistic further increase with lovastatin and cholestyramine, and a dramatic decrease with the high cholesterol diet. Spot number 413 is the most strongly regulated protein in the present experiment, showing a 5- to 10-fold induction after a 1 week treatment with 0.075% lovastatin and 1% cholestyramine in the diet (Figs. 9 and 10). Its expression follows precisely the expectation for an enzyme whose abundance is controlled by the cholesterol level; it is progressively increased from the control levels by cholestyramine, lovastatin and lovastatin plus cholestyramine, and it sinks below the threshold of detection in animals fed the high cholesterol diet. This spot has been tentatively identified as the cytosolic HMG-CoA synthase, based on a reaction with an antiserum to that protein provided by Dr. Michael Greenspan at Merck Sharp & Dohme Research Laboratories. This enzyme lies immediately before HMG-CoA reductase in the liver cholesterol biosynthesis pathway, and is known to be co-regulated with it. Spot 413 has an SDS molecular weight of about 54 000 and a CPK p*I* of −11.4, in reasonably close agreement with a molecular weight of 57 300 and a CPK p*I* of −15.7 computed from the known sequence of the hamster enzyme [43].

Using a classical product-moment correlation test (Kepler procedure CORREL), a series of five additional spots was found to be coregulated with 413. The level of correlation was exceedingly high (> 95%). Two of these, 1250 and 933, are at similar molecular weights and approximately one charge more acidic than 413 (Fig. 9), indicating that they may be covalently modified forms of the 413 polypeptide. This suspicion is strengthened by the observation that both spots are also stained by the antibody to cytosolic HMG-CoA synthase. The remaining three correlated spots appear

to comprise an additional related pair (1253 and 1001) of around 40 kDa and a single spot (1119) of around 28 kDa. Because these two presumed proteins are present at substantially lower abundances than 413, and because the cytosolic HMG-CoA synthase is reported to consist of only one type of polypeptide, they are likely to represent other, very tightly coregulated enzymes. A second group of six spots was selected based on a regulatory pattern close to the inverse of that for spot 413 (MSN's 34, 79, 178, 182, 204, 347; data not shown). For these proteins, the lowest level of expression occurs with exposure to lovastatin plus cholestyramine and the highest level upon exposure to the high-cholesterol diet. Spots 182 and 79 are highly correlated and lie about one charge apart at the same molecular weight; they may thus be isoforms of a single protein. The other four spots probably represent additional enzymes or subunits.

3.3.2 MSN 235 and coregulated spots

A third group of five spots, mainly comprised of mitochondrial proteins including putative mitochondrial HMG-CoA synthase spots, showed a modest induction by lovastatin alone, but little or no effect with any of the other treatments (including the combination of lovastatin and cholestyramine; Fig. 12). This result is intriguing because lovastatin was expected to affect only the regulation of enzymes of cholesterol synthesis, which is entirely extra-mitochondrial. Three of the spots (235, 134, 144) form a closely-packed triad at approximately 30 kDa, and are likely to represent isoforms of one protein. All three spots are stained by an antibody to the mitochondrial form of HMG-CoA synthase obtained from Dr. Greenspan. Subcellular fractionation indicates a mitochondrial location. The other two spots (633 at about 38 kDa and 724 at about 69 kDa) are each present at lower abundance than the members of the triad.

3.3.3 An example of an anti-synergistic effect

A sixth spot (367) shows strong induction by lovastatin (two- to threefold), and about half as much induction with lovastatin plus cholestyramine, but without sharing the animal-animal heterogeneity pattern of the 235-set (Fig. 13). This protein is also mitochondrial, and represents the clearest example of an anti-synergistic effect of lovastatin and cholestyramine. The existence of such an effect demonstrates that lovastatin and cholestyramine do not act exclusively through the same regulatory pathway.

3.3.4 Complexity of the cholesterol synthesis pathway

Taken together, these results suggest that treatment with lovastatin alone can affect both cytosolic and mitochondrial pathways using HMG-CoA, while cholestyramine, on the other hand, either alone or in combination with lovastatin, produces a strong effect on the putative cytosolic pathway, but little or no effect on the putative mitochondrial pathway. An explanation for this difference may lie in lovastatin's effect on levels of HMG-CoA and related precursor compounds that are exchanged between the cytosol and the mitochondrion, whereas cholestyramine should affect only the cytosolic pathways directly controlled by cholesterol and bile acid levels. It remains to be explained why some proteins of the putative mitochondrial pathway are so much more variable in their expression in all groups. An examination of all the coregulated groups suggests that quantitative statistical techniques can extract a wealth of interesting information from large sets of reproducible gels. The abundance of spots in the 413 coregulation group, for example, shows an amazing level of concordance in their relative expression among the five individuals of the lovastatin and cholestyramine treatment group. This effect is not due to differences in total protein loading, since they have already been removed by scaling, and since proteins with quite different regulation patterns can be demonstrated (*e.g.*, Fig. 13). Such effects raise the possibility that many gene coregulation sets may be revealed through the study of a sufficiently large population of control animals (*i.e.*, without any experimental manipulation). This approach, exploiting natural biological variation in protein expression instead of drug effects, offers an important incentive for the construction of a large library of control animal patterns.

4 Conclusions

Because of the widespread use of rat liver in both basic biochemistry and in toxicology, there is a long-term need for a comprehensive database of liver proteins. The rat liver master pattern presented here has proven to be an accurate representation of this system, having been matched to more than 700 gels to date. As the number of proteins identified and the number of compounds tested for gene expression effects grows, we expect this database to contribute valuable insights into gene regulation. Its practical utility in several areas of mechanistic toxicology is already being demonstrated.

Received September 11, 1991

5 References

[1] O'Farrell, P., *J. Biol. Chem.* 1975, *250*, 4007–4021.
[2] Klose, J., *Humangenetik* 1975, *26*, 231–243.
[3] Scheele, G. A., *J. Biol. Chem.* 1975, *250*, 5375–5385.
[4] Iborra, G. and Buhler, J. M., *Anal. Biochem.* 1976, *74*, 503–511.
[5] Anderson, N. G. and Anderson, N. L., *Behring. Inst. Mitt.* 1979, *63*, 169–210.
[6] Anderson, N. G. and Anderson, N. L., *Clin. Chem.* 1982, *28*, 739–748.
[7] Heydorn, W. E., Creed, G. J. and Jacobowitz, D. M., *J. Pharmacol. Exp. Therap.* 1984, *229*, 622–628.
[8] Anderson, N. L., Nance, S. L., Tollaksen, S. L., Giere, F. A. and Anderson, N. G., *Electrophoresis* 1985, *6*, 592–599.
[9] Racine, R. R. and Langley, C. H., *Biochem. Genet.* 1980, *18*, 185–197.
[10] Klose, J., *Mol. Evol.* 1982, *18*, 315–328.
[11] Neel, J. V., Baier, L., Hanash, S. and Erickson, R. P., *J. Hered.* 1985, *76*, 314–320.
[12] Marshall, R. R., Raj, A. S., Grant, F. J. and Heddle, J. A., *Can. J. Genet. Cytol.* 1983, *25*, 457–446.
[13] Taylor, J., Anderson, N. L., Anderson, N. G., Gemmell, A., Giometti, C. S., Nance, S. L. and Tollaksen, S. L., in: Dunn, M. J. (Ed.), *Electrophoresis '86*, Verlag Chemie, Weinheim 1986, pp. 583–587.
[14] Giometti, C. S., Gemmell, M. A., Nance, S. L., Tollaksen, S. L. and Taylor, J., *J. Biol. Chem.* 1987, *262*, 12764–12767.
[15] Anderson, N. L., Giere, F. A., Nance, S. L., Gemmell, M. A., Tollaksen, S. L. and Anderson, N. G., in: Galteau, M.-M. and Siest, G. (Eds.), *Progrès Récents en Electrophorèse Bidimensionelle*, Presses Universitaires de Nancy, Nancy 1986, pp. 253–260.
[16] Anderson, N. L., Swanson, M., Giere, F. A., Tollaksen, S., Gemmell, A., Nance, S. L. and Anderson, N. G., *Electrophoresis* 1986, *7*, 44–48.

[17] Anderson, N. L., Giere, F. A., Nance, S. L., Gemmell, M. A., Tollaksen, S. L. and Anderson, N. G., *Fundam. Appl. Toxicol.* 1987, *8*, 39–50.
[18] Anderson, N. L., in: *New Horizons in Toxicology*, Eli Lilly Symposium, 1991, in press.
[19] Antoine, B., Rahimi-Pour, A., Siest, G., Magdalou, J. and Galteau, M. M., *Cell. Biochem. Funct.* 1987, *5*, 217–231.
[20] Elliott, B. M., Ramasamy, R., Stonard, M. D. and Spragg, S. P. *Biochim. Biophys. Acta* 1986, *870*, 135–140.
[21] Huber, B. E., Heilman, C. A., Wirth, P. J., Miller, M. J. and Thorgeirsson, S. S., *Hepatology* 1986, *6*, 209–219.
[22] Wirth, P. J. and Vesterberg, O., *Electrophoresis* 1988, *9*, 47–53.
[23] Witzmann, F. A. and Parker, D. N., *Toxicol. Lett.* 1991, *57*, 29–36.
[24] Rampersaud, A., Waxman, D. J., Ryan, D. E., Levin, W. and Walz, F. G., Jr., *Arch. Biochem. Biophys.* 1985, *243*, 174–183.
[25] Vlasuk, G. P. and Walz, F. G., Jr., *Anal. Biochem.* 1980, *105*, 112–120.
[26] Anderson, N. G. and Anderson, N. L., *Anal. Biochem.* 1978, *85*, 331–340.
[27] Anderson, N. L. and Anderson, N. G., *Anal. Biochem.* 1978, *85*, 341–354.
[28] Anderson, L., Hofmann, J.-P., Anderson, E., Walker, B. and Anderson, N. G., in: Endler, A. T. and Hanash, S. (Eds.), *Two-Dimensional Electrophoresis*, VCH Verlagsgesellschaft, Weinheim 1989, pp. 288–297.
[29] Anderson, L., *Two-Dimensional Electrophoresis: Operation of the ISO-DALT® System*. Large Scale Biology Press, Washington, DC 1988, ISBN 0-945532-00-8, 170pp.
[30] Neuhoff, V., Stamm, R. and Eibl, H., *Electrophoresis* 1985, *6*, 427–448.
[31] Neuhoff, V., Arold, N., Taube, D. and Ehrhardt, W., *Electrophoresis* 1988, *9*, 255–262.
[32] Anderson, N. L. and Hickman, B. J., *Anal. Biochem.* 1979, *93*, 312–320.
[33] Sidman, K. E., George, D. E., Barker, W. C. and Hunt, L. T., *Nucl. Acids Res.* 1988, *16*, 1869–1871.
[34] Taylor, J., Anderson, N. L., Coulter, B. P., Scandora, A. E. and Anderson, N. G., in: Radola, B. J. (Ed.), *Electrophoresis '79*, de Gruyter, Berlin 1980, pp. 329–339.
[35] Taylor, J., Anderson, N. L. and Anderson, N. G., in: Allen, R. C. and Arnaud, P. (Eds.), *Electrophoresis '81*, de Gruyter, Berlin 1981, pp. 383–400.
[36] Anderson, N. L., Taylor, J., Scancora, A. E., Coulter, B. P. and Anderson, N. G., *Clin. Chem.* 1981, *27*, 1807–1820.
[37] Taylor, J., Anderson, N. L., Scandora, A. E., Jr., Willard, K. E. and Anderson, N. G., *Clin. Chem.* 1982, *28*, 861–866.
[38] Taylor, J., Anderson, N. L. and Anderson, N. G., *Electrophoresis* 1983, *4*, 338–345.
[39] Anderson, N. L. and Taylor, J., in: *Proceedings of the Fourth Annual Conference and Exposition of the National Computer Graphics Association*, Chicago, June 26–30, 1983, pp. 69–76.
[40] Anderson, N. L., Hofmann, J.-P., Gemmell, A. and Taylor, J., *Clin. Chem.* 1984, *30*, 2031–2036.
[41] Anderson, L., in: Schafer-Nielsen, C. (Ed.), *Electrophoresis '88*, VCH Verlagsgesellschaft, Weinheim 1988, pp. 313–321.
[42] Neidhardt, F. C., Appleby, D. A., Sankar, P., Hutton, M. E. and Phillips, T. A., *Electrophoresis* 1989, *10*, 116–121.
[43] Gil, G., Goldstein, J. L., Slaughter, C. A. and Brown, M. S., *J. Biol. Chem.* 1986, *261*, 3710–3716.

6 Addendum 1: Figures 1–13

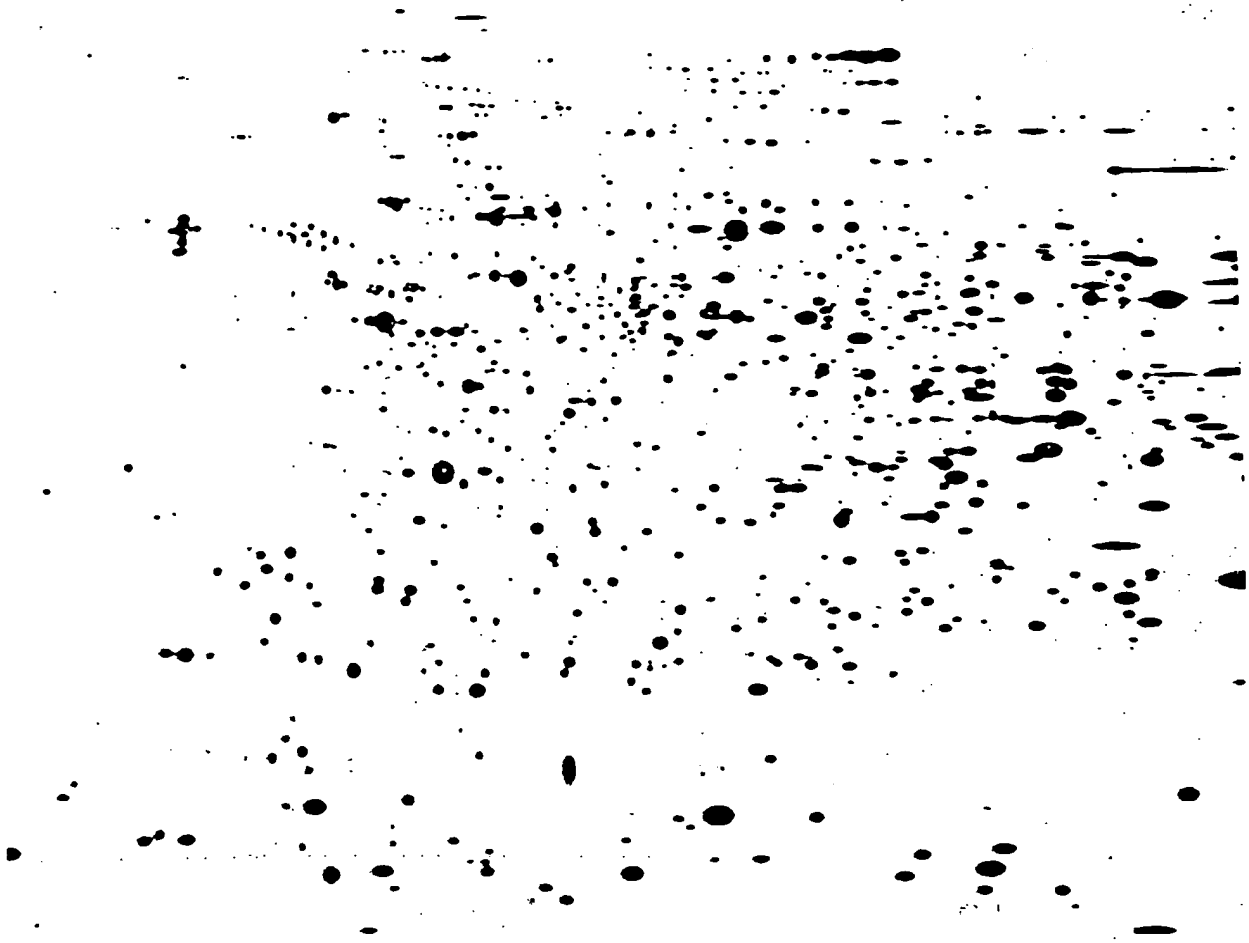

Figure 1. Synthetic representation of the standard rat liver 2-D master pattern, rendered as a greyscale image using a videoprinter.

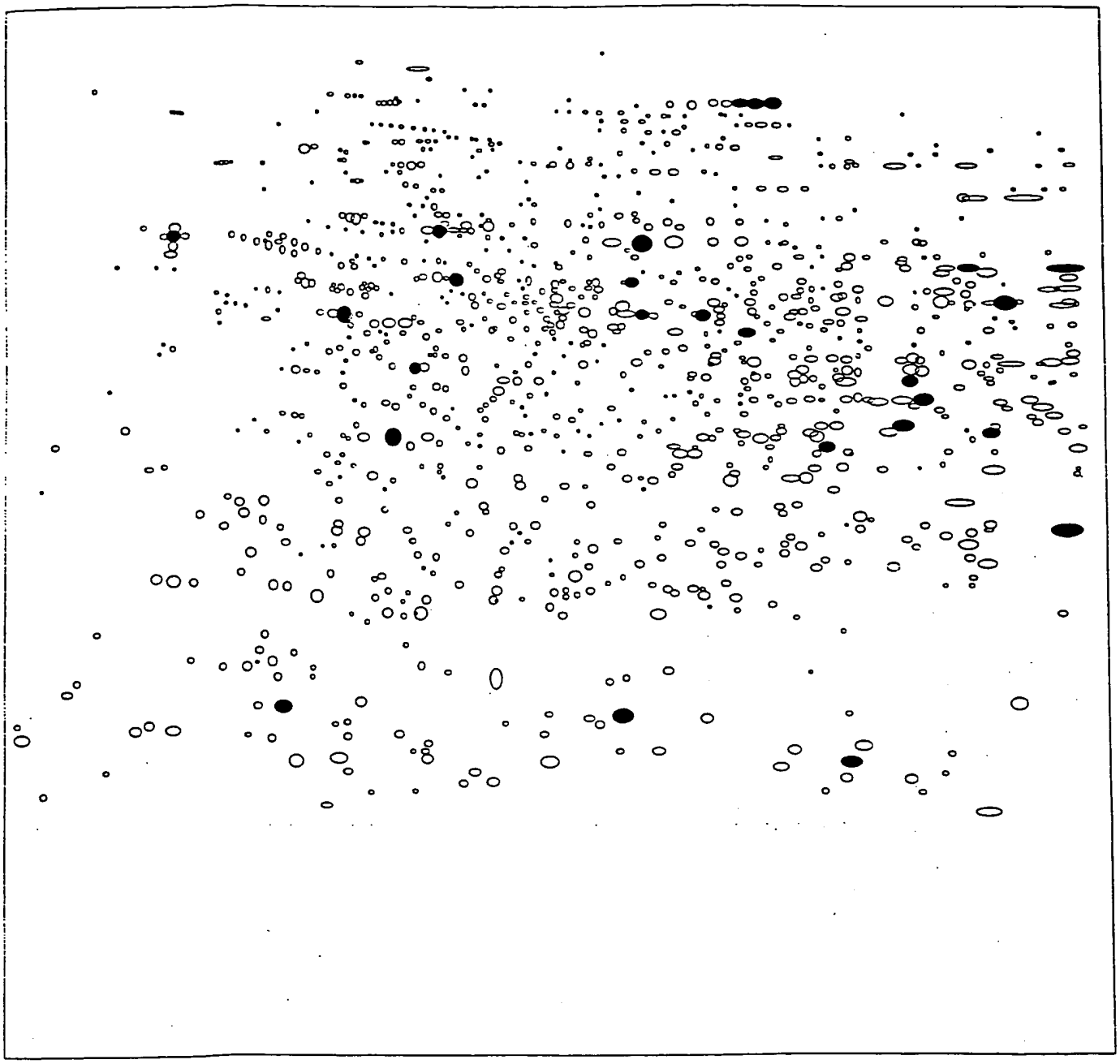

Figure 2. Schematic representation of the master pattern (the same as Fig. 1), useful as an aid in relating specific areas of Fig. 1 and the following detailed quadrants.

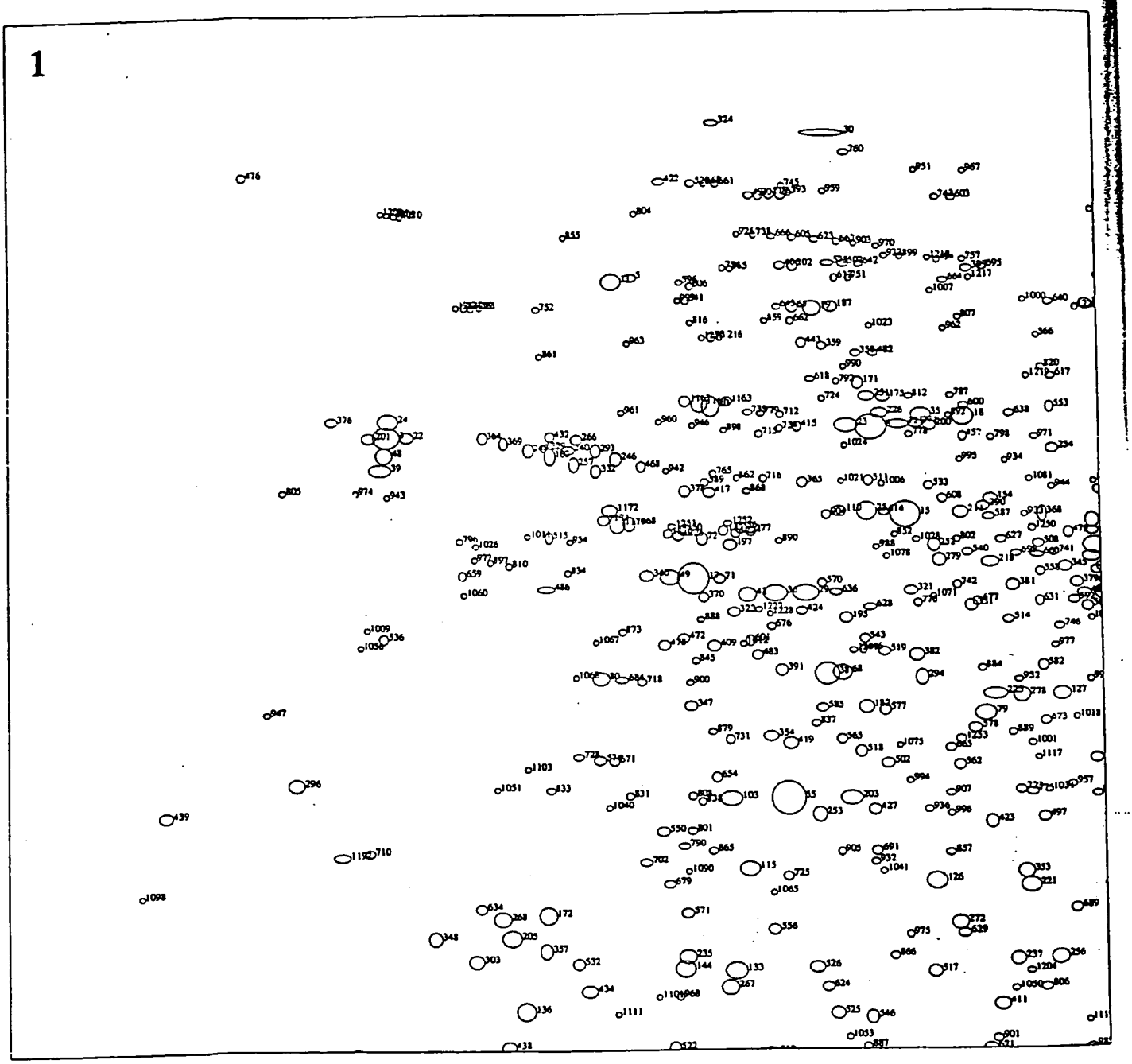

Figure 3. Upper left (high molecular weight, acidic) quadrant (#1) of the rat liver map, showing spot numbers.

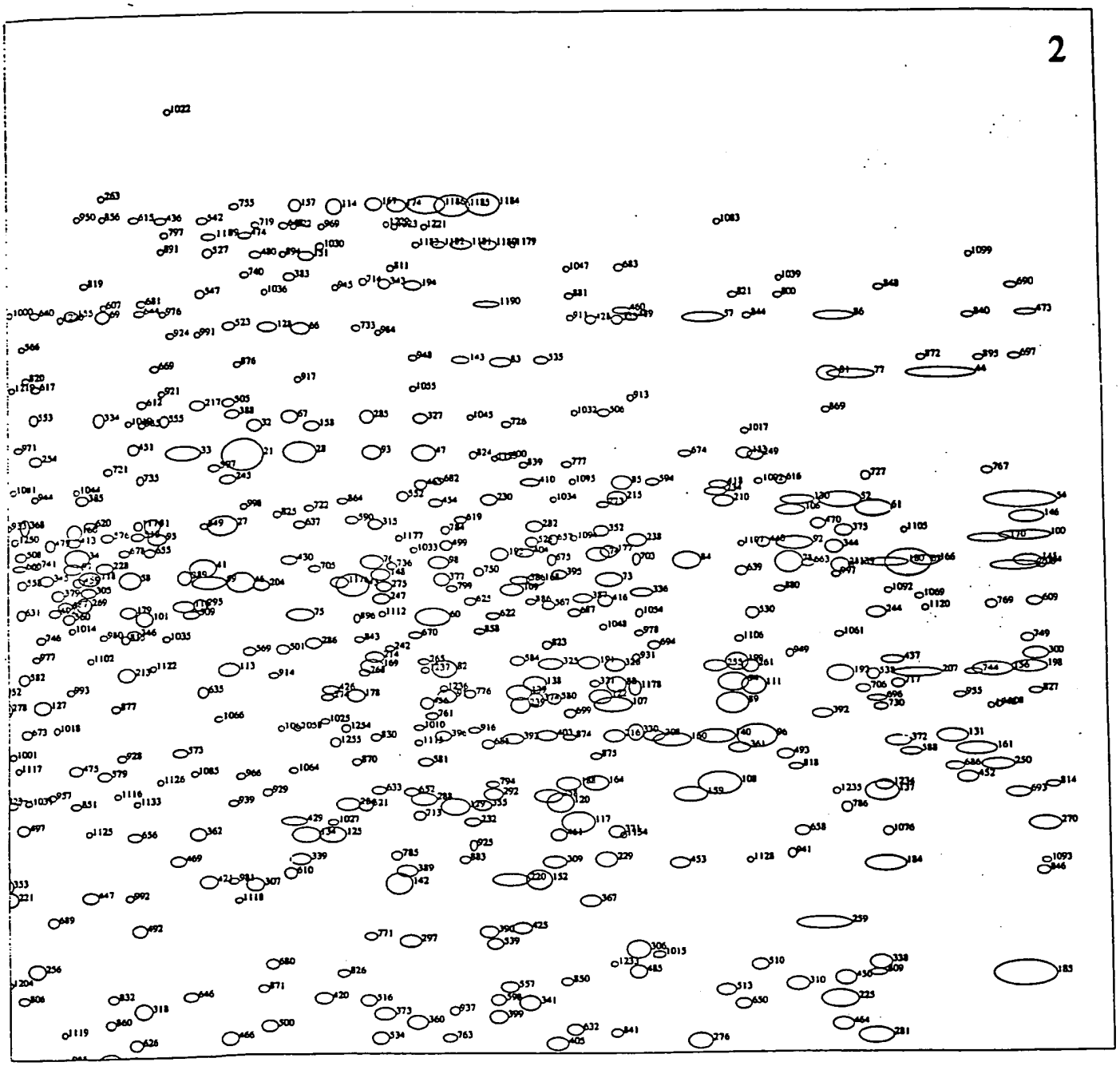

Figure 4. Upper right (high molecular weight, basic) quadrant (#2) of the rat liver map, showing spot numbers.

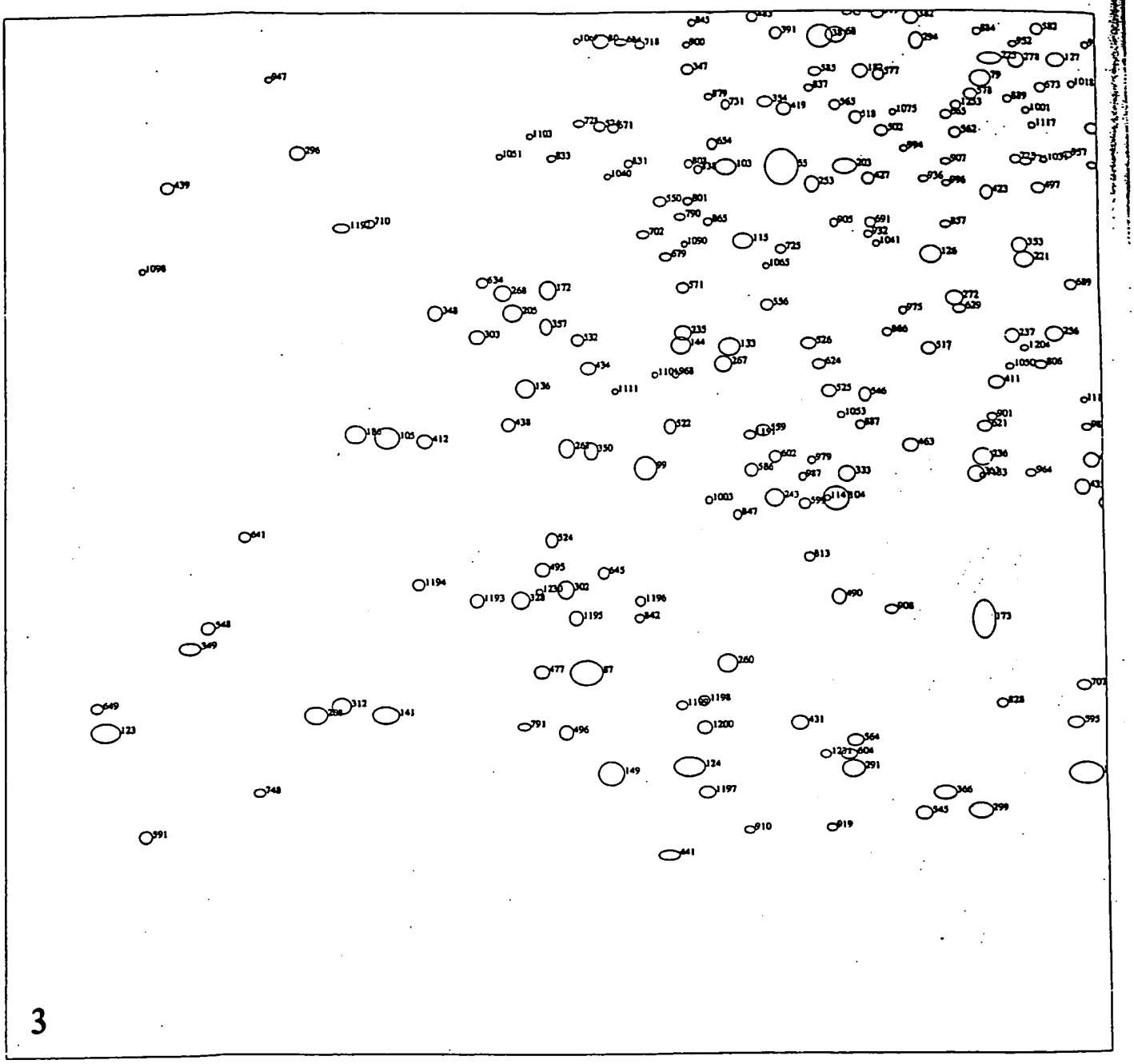

Figure 5. Lower left (low molecular weight, acidic) quadrant (#3) of the rat liver map, showing spot numbers.

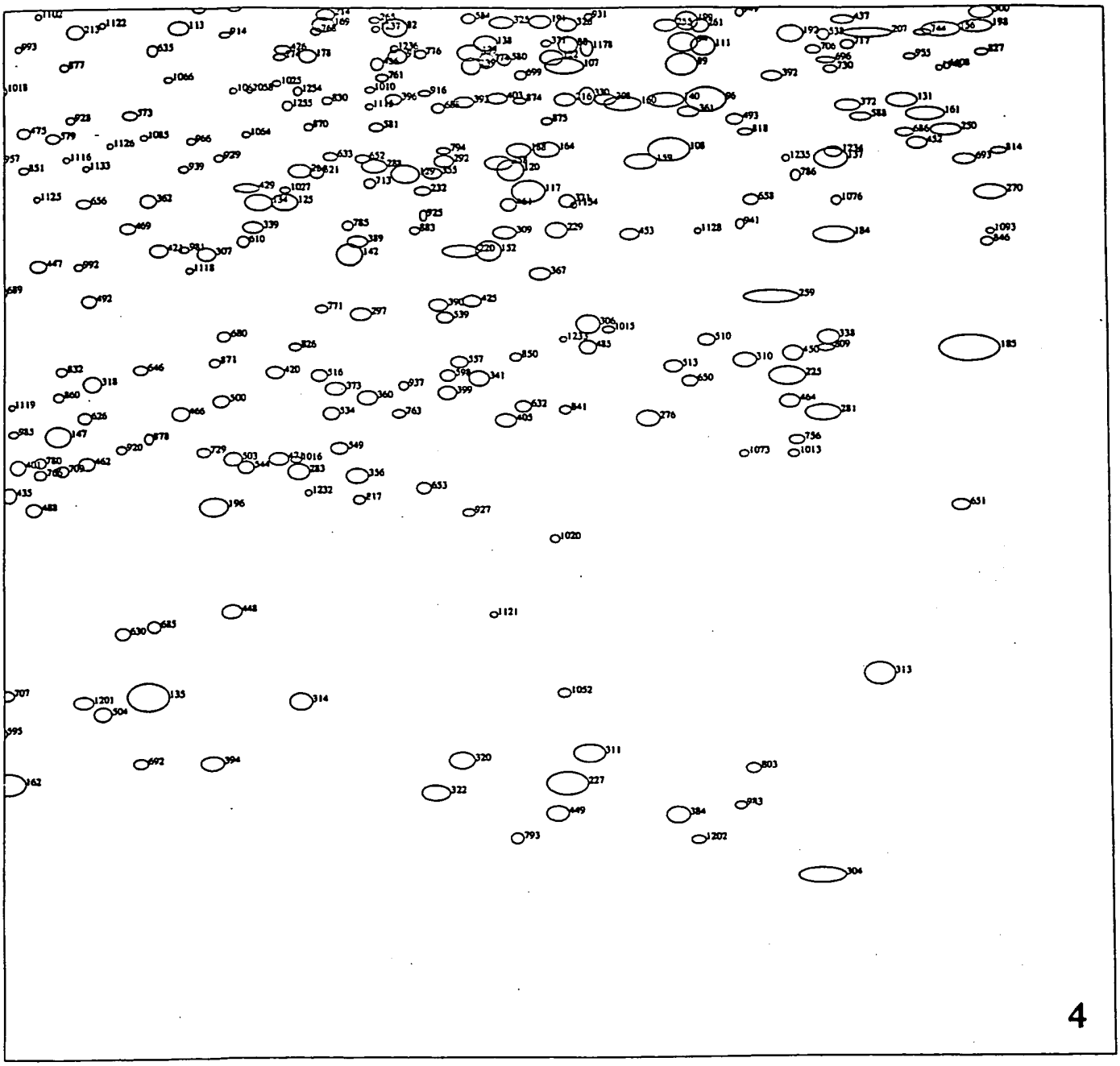

Figure 6. Lower right (low molecular weight, basic) quadrant (#4) of the rat liver map, showing spot numbers.

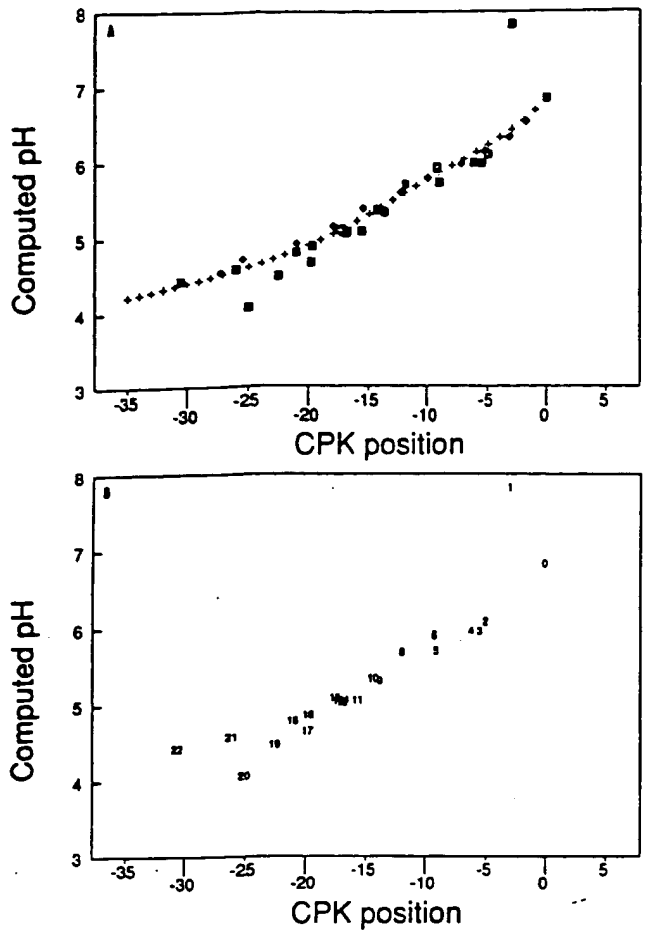

◀ *Figure 7.* (a) Plot of computed isoelectric point versus gel *X*-position for two sets of carbamylated standard proteins (rabbit muscle CPK [+] and human hemoglobin β chain, filled diamonds) and several other proteins (shaded squares). (b) The identities of the various proteins represented by the squares are indicated by the numbers in corresponding positions on (a); these refer to Table 4.

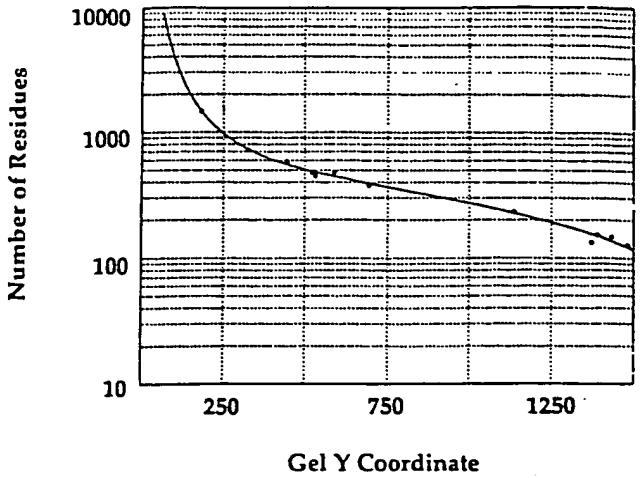

Figure 8. Plot of number of amino acids versus gel *Y*-position, with fitted curve used to predict molecular mass of unidentified proteins.

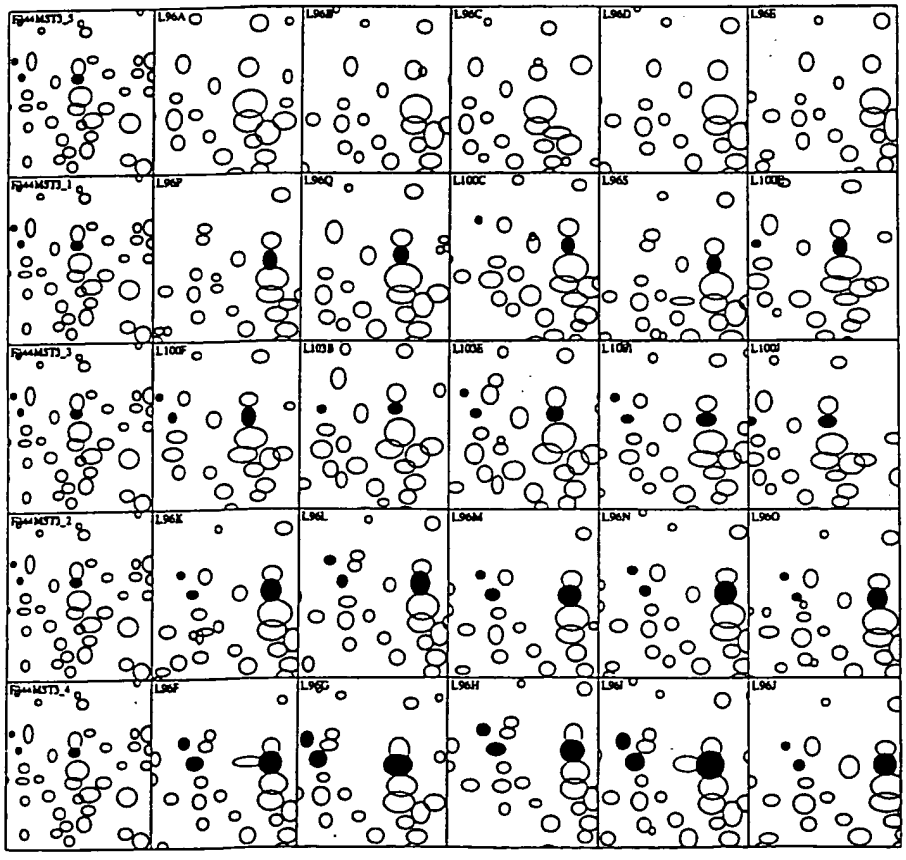

Figure 9. Montage showing effects in the region of MSN:413. The montage shows a small window into one portion of the 2-D pattern, one row of windows for each experimental group, and one panel for each gel in the experiment. The left-most pattern in each row is a group-specific copy of the master pattern followed by the patterns for the five individual rats in the group. The highlighted protein spots (filled circles) are spot 413 (on the right of each panel; identified as cytosolic HMG-CoA synthase) and two modified forms of it (1250 and 933). From the top, the rows (experimental groups) are: high cholesterol, controls, cholestyramine, lovastatin, and lovastatin plus cholestyramine.

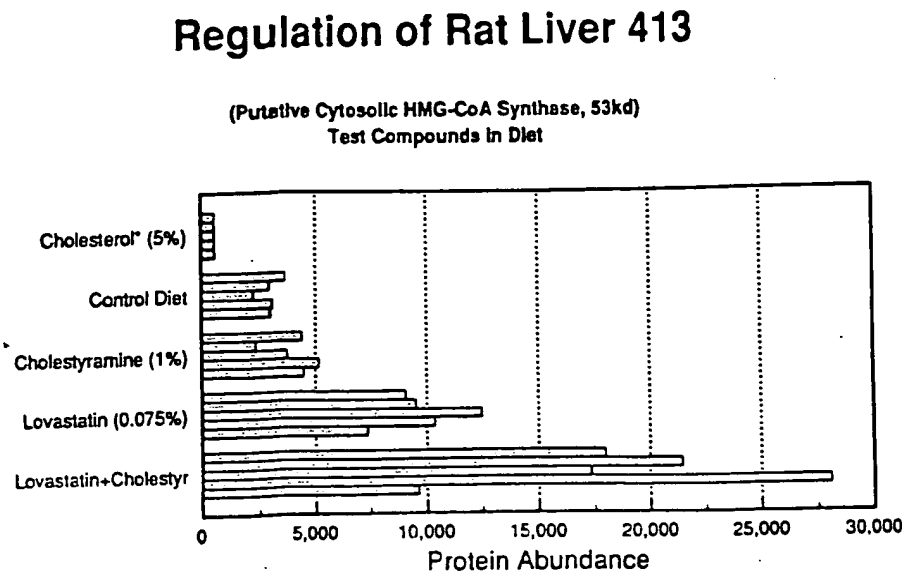

Figure 10. Bargraph showing the quantitative effects of various treatments on the abundance of MSN:413 (cytosolic HMG-CoA synthase) in the gels of Fig. 9.

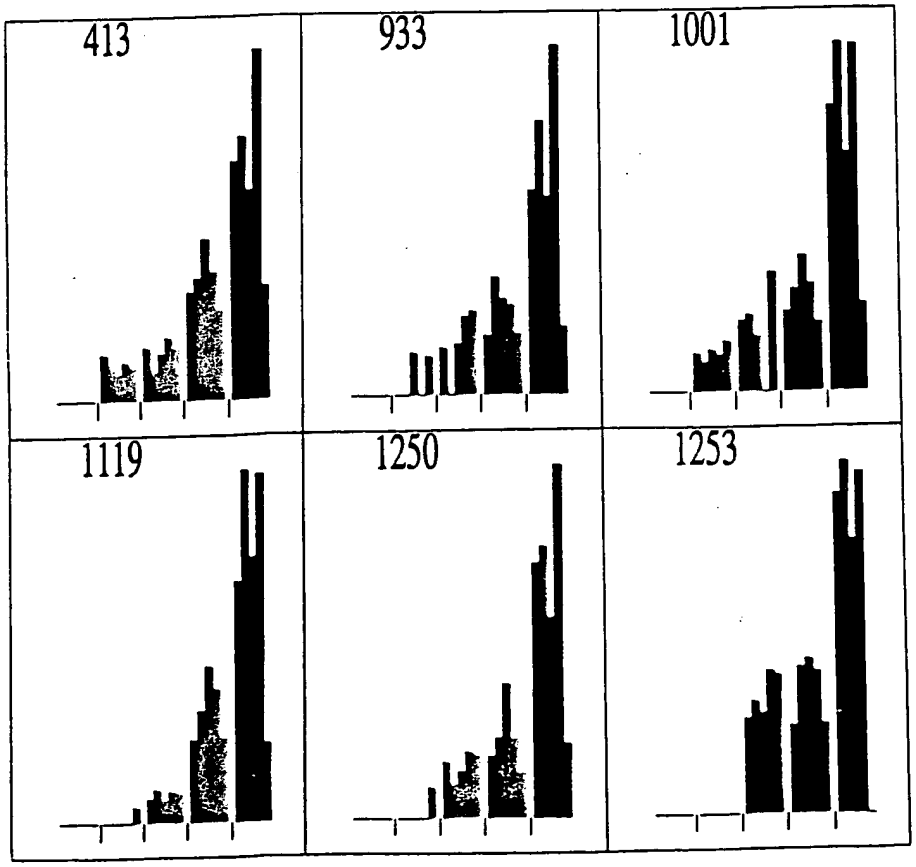

Figure 11. Bargraphs of a series of six coregulated spots including MSN:413. In the bargraphs, the abundances of the appropriate spot (master spot number shown at the top of the panel) in each animal are shown. The five five-animal groups are in the order (left to right): high cholesterol, controls, cholestyramine, lovastatin, and lovastatin plus cholestyramine. Each bar within a group represents one experimental animal liver (one 2-D gel). Note the correlated expression of the 6 spots, especially in the two far right (most strongly induced) groups.

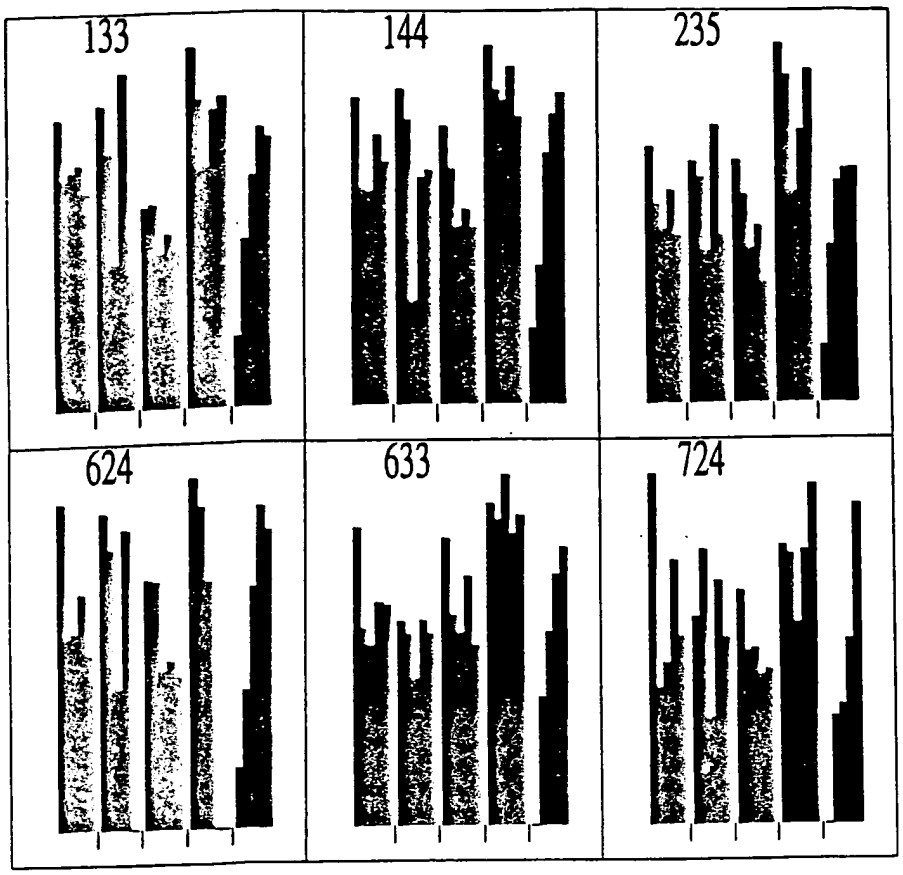

Figure 12. Data on a second coregulated group of spots, presented as in Fig. 11. The fourth experimental group (lovastatin) shows a modest induction, while the fifth group (lovastatin plus cholestyramine) does not.

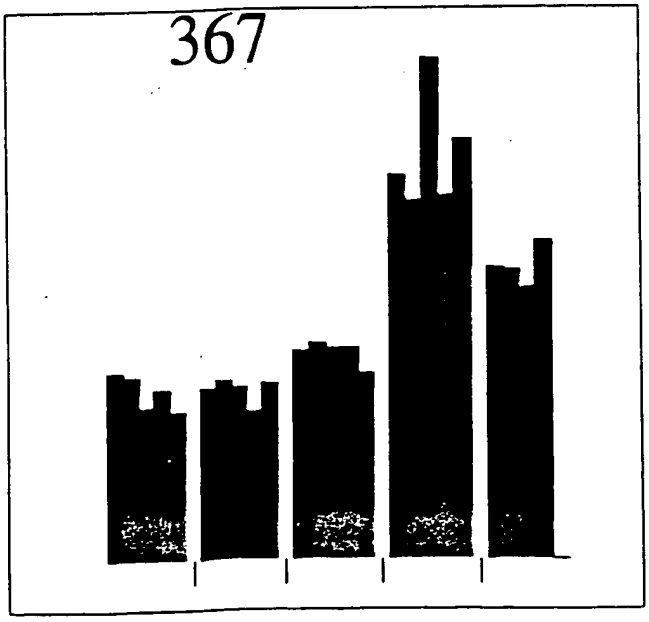

Figure 13. Data on spot MSN:367, presented as in Fig. 11. This protein shows unambiguously the anti-synergistic effect of lovastatin and cholestyramine (fifth group) as compared to lovastatin (fourth group). This response contrasts strongly with the regulation pattern seen in Fig. 11.

Table 1. Master table of proteins in the rat liver database[a)]

MSN	X	Y	CPKpI	SDSMW	MSN	X	Y	CPKpI	SDSMW	MSN	X	Y	CPKpI	SDSMW
3	311	434	<-35.0	63,800	95	1119	536	-9.9	53,800	174	1364	183	-6.7	162,900
5	568	263	-24.3	102,900	96	1731	756	-2.0	40,700	175	825	393	-15.7	69,300
8	812	426	-16.0	64,800	97	1033	566	-11.4	51,600	177	1582	553	-3.6	52,600
11	549	268	-25.2	101,000	98	1406	565	-6.1	51,700	178	1321	710	-7.2	43,000
15	845	520	-15.3	55,200	99	578	1149	-23.8	25,000	179	1089	615	-10.4	48,300
17	629	589	-21.6	50,000	100	2004	538	>0.0	53,700	180	1866	567	-0.5	51,600
18	906	414	-14.0	66,300	101	1106	623	-10.1	47,900	181	411	295	-32.1	91,200
19	755	298	-17.5	90,200	102	482	455	-28.5	61,300	182	804	730	-16.2	42,000
20	649	403	-20.9	67,900	103	665	830	-20.2	37,300	184	1860	896	-0.6	34,500
21	1204	448	-8.7	62,100	104	773	1182	-17.0	23,800	185	1997	1017	>0.0	29,800
22	332	434	<-35.0	63,800	105	312	1117	<-35.0	26,100	186	279	1113	<-35.0	26,300
23	787	424	-16.6	65,000	106	1769	509	-1.5	56,100	187	773	296	-17.0	90,800
24	313	417	<-35.0	66,000	107	1585	720	-3.6	42,500	188	1538	807	-4.2	38,400
25	807	516	-16.1	55,500	108	1692	807	-2.4	38,300	191	1560	674	-3.9	44,900
27	1184	524	-9.0	54,900	109	1482	593	-4.8	49,700	192	1818	687	-0.9	44,200
28	1263	446	-8.0	62,400	110	778	516	-16.9	55,500	193	1469	555	-5.0	52,400
29	743	605	-17.8	49,000	111	1728	700	-2.0	43,500	194	1380	266	-6.4	101,600
30	768	112	-17.2	348,600	113	1191	680	-8.9	44,500	195	784	632	-16.7	47,300
32	1216	417	-8.6	66,000	114	1298	185	-7.5	160,800	196	1227	1185	-8.4	23,700
33	1145	445	-9.5	62,500	115	682	907	-19.6	34,100	197	667	553	-20.1	52,600
34	1037	555	-11.3	52,400	116	1146	610	-9.5	48,700	198	2006	681	>0.0	44,500
35	863	412	-14.9	66,600	117	1548	849	-4.1	36,500	199	1711	674	-2.2	44,900
36	712	606	-18.7	48,900	118	1050	577	-11.1	50,800	200	872	424	-14.7	65,000
38	763	694	-17.3	43,800	120	1530	828	-4.3	37,400	201	292	435	<-35.0	63,700
39	304	470	<-35.0	59,800	121	638	423	-15.4	65,200	202	736	253	-18.0	107,800
41	1165	569	-9.2	51,400	122	1572	712	-3.8	42,900	203	786	829	-16.7	37,400
42	684	607	-19.6	48,800	123	23	1433	<-35.0	15,300	204	1224	589	-8.5	50,000
43	1318	589	-7.3	50,000	124	621	1474	-21.9	13,900	205	439	983	-30.9	31,100
44	1924	362	-0.1	74,600	125	1298	862	-7.5	36,000	206	1994	571	>0.0	51,300
46	1203	586	-8.7	50,200	126	872	921	-14.7	33,500	207	1895	687	-0.3	44,200
47	1391	447	-6.3	62,300	127	1000	717	-12.0	42,600	208	240	1418	<-35.0	15,800
48	309	454	<-35.0	61,500	128	1229	311	-8.4	86,100	210	1700	499	-2.3	57,000
49	605	587	-22.5	50,100	129	1422	832	-5.8	37,300	211	902	517	-14.1	55,400
50	621	535	-21.8	53,900	130	1776	499	-1.4	57,000	213	1087	684	-10.4	44,400
51	1113	522	-10.0	55,000	131	1930	757	-0.1	40,700	214	1340	668	-7.0	45,200
52	1820	499	-0.9	57,000	132	660	537	-20.4	53,800	215	1591	495	-3.5	57,300
53	725	177	-18.3	170,800	133	666	1019	-20.2	29,700	216	1585	755	-3.6	40,700
54	2001	500	>0.0	56,900	134	1271	862	-7.9	36,000	217	1159	393	-9.3	69,300
55	722	830	-18.4	37,300	135	1161	1389	-9.3	16,800	218	931	572	-13.5	51,200
56	678	533	-19.8	54,100	136	453	1063	-29.7	28,100	219	713	177	-18.7	170,500
57	1682	302	-2.5	89,000	137	1858	823	-0.6	37,700	220	1479	911	-4.9	33,900
58	1091	580	-10.3	50,600	138	1504	697	-4.6	43,700	221	965	927	-12.8	33,300
59	1171	585	-9.2	50,300	139	1488	707	-4.8	43,200	223	934	716	-13.5	42,700
60	1400	624	-6.2	47,800	140	1689	756	-2.4	40,700	225	1812	1045	-1.0	28,800
61	1853	508	-0.6	56,200	141	311	1417	<-35.0	15,800	226	821	411	-15.8	66,800
62	1888	567	-0.4	51,500	142	1366	915	-6.7	33,800	227	1586	1483	-3.6	13,600
65	735	297	-18.1	90,500	143	1429	346	-5.7	77,900	228	1065	567	-10.8	51,600
66	1263	312	-8.0	85,900	144	615	1017	-22.1	29,800	229	1577	890	-3.7	34,800
67	1252	407	-8.1	67,300	145	2006	566	>0.0	51,600	230	1458	496	-5.2	57,300
68	779	692	-16.8	43,900	146	2006	518	>0.0	55,300	232	1440	849	-5.5	36,500
69	1064	296	-10.8	90,800	147	1070	1108	-10.7	26,500	234	1692	489	-2.4	57,900
71	656	589	-20.6	50,000	148	1347	578	-6.9	50,800	235	618	1004	-22.0	30,300
72	638	545	-21.2	53,100	149	541	1481	-25.7	13,700	236	920	1138	-13.7	25,400
73	1582	583	-3.6	50,400	150	1645	760	-2.8	40,500	237	952	1008	-13.1	30,200
74	1570	556	-3.8	52,300	151	1269	236	-7.9	117,000	238	1611	541	-3.2	53,500
75	1264	621	-8.0	48,000	152	1507	911	-4.5	33,900	239	1489	720	-4.8	42,500
76	1338	564	-7.0	51,800	153	1722	448	-2.1	62,100	240	501	448	-27.7	62,100
77	1833	363	-0.8	74,400	154	932	503	-13.5	56,600	241	1820	569	-0.9	51,400
78	1767	565	-1.5	51,700	155	1031	294	-11.4	91,400	242	1357	658	-6.8	45,800
79	925	738	-13.6	41,600	156	1970	684	>0.0	44,400	243	711	1182	-18.7	23,800
80	534	698	-26.1	43,600	157	1258	183	-8.1	162,400	244	1855	621	-0.6	48,000
81	1811	363	-1.0	74,500	158	1275	417	-7.8	65,900	245	1189	474	-8.9	59,300
82	1412	681	-6.0	44,500	159	1663	820	-2.6	37,800	246	551	459	-25.1	61,000
83	1471	347	-5.0	77,500	160	1034	527	-11.4	54,600	247	1348	604	-6.9	49,100
84	1662	563	-2.7	51,800	161	1953	771	>0.0	40,000	248	460	448	-29.3	62,100
85	1596	479	-3.4	58,900	162	1020	1482	-11.6	13,700	249	1733	451	-1.9	61,800
86	1817	301	-0.9	89,100	164	1566	806	-3.8	38,400	250	1974	788	>0.0	39,200
87	516	1371	-27.0	17,400	166	1905	565	-0.2	51,700	251	808	392	-16.1	69,500
88	1589	698	-3.5	43,600	167	1340	181	-7.0	164,900	252	874	553	-14.6	52,500
89	1706	719	-2.2	42,500	168	1506	583	-4.6	50,400	253	753	848	-17.6	36,500
90	651	329	-20.8	81,700	169	1338	678	-7.0	44,700	254	995	450	-12.1	61,900
91	1415	710	-6.0	43,000	170	1969	541	>0.0	53,500	255	1690	679	-2.4	44,600
92	1773	545	-1.4	53,200	171	800	378	-16.3	71,800	256	994	1006	-12.1	30,200
93	1338	446	-7.0	62,300	172	476	958	-28.7	32,100	257	508	464	-27.4	60,400
94	1708	696	-2.2	43,700	173	919	1314	-13.7	19,300	258	1517	820	-4.4	37,800

[a)] Master table of proteins in the rat liver database, showing spot master number, gel position (x and y), isoelectric point relative to CPK standards, and predicted molecular mass (from the standard curve of Fig. 8).

MSN	X	Y	CPKpl	SDSMW
259	1796	961	-1.1	31,900
260	661	1361	-20.4	17,700
261	1725	679	-2.0	44,600
262	496	1127	-28.0	25,800
263	1063	172	-10.9	177,400
265	1390	673	-6.3	45,000
266	510	437	-27.3	63,400
267	660	1038	-20.4	29,000
268	430	961	-31.0	31,900
269	1044	606	-11.2	48,900
270	2019	853	>0.0	36,300
271	857	422	-15.0	65,200
272	895	968	-14.2	31,700
274	1292	712	-7.6	42,900
275	1350	590	-6.9	49,900
276	1670	1089	-2.6	27,100
277	688	538	-19.4	53,700
278	961	718	-13.0	42,600
279	879	570	-14.5	51,300
281	1848	1084	-0.7	27,300
282	1505	525	-4.6	54,800
283	1313	1147	-7.3	25,100
284	1314	829	-7.3	37,400
285	1332	408	-7.1	67,200
286	1277	652	-7.8	46,100
288	1391	824	-6.3	37,600
289	1147	579	-9.5	50,700
290	925	511	-13.6	55,900
291	787	1476	-16.6	13,900
292	1462	818	-5.1	37,800
293	531	449	-26.3	62,000
294	860	698	-14.9	43,600
295	1162	609	-9.3	48,700
296	218	814	<-35.0	38,000
297	1377	979	-6.5	31,300
299	913	1523	-13.9	12,400
300	2012	667	>0.0	45,300
301	702	178	-19.0	169,200
302	494	1280	-28.1	20,400
303	403	1008	-32.6	30,100
304	1843	1585	-0.7	10,300
305	1049	593	-11.1	49,800
306	1608	989	-3.3	30,900
307	1219	916	-8.5	33,700
308	1627	755	-3.0	40,700
309	1524	892	-4.4	34,700
310	1769	1028	-1.5	29,400
311	1609	1451	-3.3	14,700
312	266	1408	<-35.0	16,100
313	1902	1365	-0.3	17,600
314	1316	1395	-7.3	16,600
315	1341	523	-7.0	54,900
318	1104	1053	-10.1	28,500
320	1480	1459	-4.9	14,400
321	850	603	-15.1	49,100
322	1454	1494	-5.3	13,300
323	670	626	-20.0	47,700
324	655	101	-20.6	420,500
325	1521	675	-4.4	44,800
326	1587	677	-3.6	44,700
327	1388	409	-6.3	67,000
328	448	1291	-30.0	20,100
330	1608	751	-3.3	40,900
331	1566	697	-3.8	43,700
332	531	471	-26.3	59,600
333	784	1156	-16.7	24,700
334	1059	407	-10.9	67,300
335	1593	303	-3.5	88,500
336	1616	598	-3.2	49,400
338	1854	1004	-0.6	30,300
339	1265	888	-8.0	34,900
340	581	585	-23.6	50,300
341	1497	1047	-4.7	28,700
343	1351	265	-6.8	102,200
344	1813	549	-0.9	52,800
345	1006	578	-11.9	50,800
346	1095	640	-10.3	46,800
347	625	728	-21.7	42,000
348	361	983	-35.3	31,100
349	110	1343	<-35.0	18,300
350	521	1130	-26.7	25,700
351	912	619	-13.9	48,100
352	1574	530	-3.7	54,300
353	961	912	-12.9	33,900
354	706	762	-18.9	40,400
355	1450	830	-5.3	37,300
356	1374	1152	-6.5	24,900
357	474	997	-28.7	30,600
358	798	346	-16.3	77,800
359	764	338	-17.3	79,400
360	1384	1068	-6.4	27,900
361	1713	769	-2.1	40,100
362	1161	859	-9.3	36,100
363	914	1156	-13.8	24,800
364	412	435	-32.0	63,700
365	741	486	-17.9	58,200
366	878	1503	-14.6	13,000
367	1560	935	-3.9	33,000
368	983	520	-12.4	55,200
369	434	441	-31.0	63,000
370	639	610	-21.2	48,700
371	1587	860	-3.6	36,100
372	1875	762	-0.5	40,400
373	1351	1059	-6.8	28,300
374	1506	715	-4.6	42,700
375	1823	532	-0.9	54,200
376	254	417	<-35.0	65,900
377	1409	583	-6.1	50,400
378	621	494	-21.8	57,500
379	1017	595	-11.7	49,600
381	953	598	-13.1	49,400
382	856	674	-15.0	44,900
383	1252	258	-8.1	105,300
384	1699	1518	-2.3	12,500
385	1042	493	-11.2	57,500
386	1490	583	-4.7	50,400
387	1554	603	-4.0	49,100
388	1193	404	-8.9	67,700
389	1374	902	-6.5	34,300
390	1456	969	-5.2	31,700
391	718	690	-18.5	44,000
392	1799	732	-1.1	41,900
393	1482	758	-4.8	40,600
394	1227	1461	-8.4	14,400
395	1530	577	-4.3	50,800
396	1410	755	-6.0	40,800
397	912	256	-13.9	106,400
399	1465	1063	-5.0	28,100
400	1473	450	-4.9	61,900
401	1029	1140	-11.5	25,300
403	1516	754	-4.4	40,800
404	1495	554	-4.7	52,500
405	1525	1092	-4.3	27,100
406	723	252	-18.4	108,000
409	650	663	-20.8	45,500
410	1501	478	-4.6	59,000
411	936	1057	-13.4	28,300
412	350	1120	-35.9	26,000
413	1033	538	-11.4	53,700
415	737	425	-18.0	64,900
416	1578	606	-3.7	48,900
417	646	496	-21.0	57,300
418	1695	482	-2.3	58,600
419	725	770	-18.3	40,000
420	1289	1041	-7.7	28,900
421	1171	912	-9.1	33,900
422	599	162	-22.8	193,700
423	929	856	-13.6	36,200
424	739	625	-17.9	47,700
425	1490	965	-4.7	31,800
426	1296	704	-7.6	43,300
427	810	843	-16.0	36,800
428	1565	303	-3.9	88,700
429	1259	847	-8.0	36,600
430	1253	562	-8.1	51,900
431	734	1426	-18.1	15,500
432	483	433	-28.5	63,900
434	518	1041	-26.9	28,900
435	1020	1170	-11.6	24,300
436	1122	196	-9.8	147,600
437	1870	673	-0.5	45,000
438	435	1102	-31.0	26,700
439	86	847	<-35.0	36,600
440	1740	544	-1.8	53,200
441	599	1571	-22.8	10,800
443	743	335	-17.8	80,100
446	801	668	-16.2	45,200
447	1050	926	-11.1	33,300
448	1245	1298	-8.2	19,800
449	1576	1516	-3.7	12,600
450	1818	1021	-0.9	29,600
451	1094	440	-10.3	63,100
452	1945	802	>0.0	38,600
453	1652	894	-2.8	34,600
454	1403	500	-6.1	56,900
456	1394	718	-6.3	42,600
457	905	436	-14.0	63,500
459	1038	581	-11.3	50,500
460	1598	294	-3.4	91,400
461	1528	863	-4.3	35,900
462	1098	1137	-10.2	25,400
463	849	1125	-15.2	25,800
464	1814	1072	-0.9	27,800
465	1388	481	-6.3	58,700
466	1194	1084	-8.9	27,300
468	577	467	-23.9	60,100
469	1140	888	-9.6	34,900
470	1797	524	-1.1	54,800
471	1293	1133	-7.6	25,500
472	618	655	-21.9	46,000
473	2009	299	>0.0	89,900
474	1205	215	-8.7	131,300
475	1035	788	-11.4	39,200
476	160	155	<-35.0	207,600
477	469	1370	-28.9	17,400
478	599	662	-22.8	45,600
479	1009	540	-11.8	53,500
480	1216	235	-8.6	117,400
482	816	346	-15.9	77,800
483	693	673	-19.3	44,900
485	1608	1013	-3.3	30,000
486	478	599	-28.6	49,300
487	1025	607	-11.5	48,800
488	1045	1186	-11.2	23,700
489	1609	301	-3.3	89,200
490	775	1289	-17.0	20,100
491	692	178	-19.3	169,300
492	1100	964	-10.2	31,800
493	1760	776	-1.6	39,700
494	882	247	-14.5	110,700
495	470	1258	-28.9	21,200
496	494	1436	-28.1	15,200
497	980	852	-12.5	36,400
499	1414	546	-6.0	53,100
500	1234	1072	-8.3	27,800
501	1246	659	-8.2	45,700
502	824	792	-15.7	39,000
503	1246	1134	-8.2	25,500
504	1115	1407	-9.9	16,200
505	1189	391	-8.9	69,700
506	1578	402	-3.7	68,000
507	787	250	-16.6	109,000
508	979	552	-12.5	52,600
509	1153	619	-9.4	48,100
510	1730	1006	-2.0	30,200

MSN	X	Y	CPKpI	SDSMW
511	809	484	-16.0	58,400
512	1099	533	-10.2	54,100
513	1696	1034	-2.3	29,200
514	948	636	-13.2	47,100
515	481	543	-28.5	53,400
516	1334	1044	-7.1	26,800
517	868	1021	-14.8	29,700
518	798	779	-16.3	39,600
519	822	670	-15.7	45,100
520	632	165	-21.5	189,000
521	1332	830	-7.1	37,300
522	603	1104	-22.6	26,600
523	1190	309	-8.9	86,800
524	479	1226	-28.6	22,300
525	768	1066	-17.2	28,000
526	747	1016	-17.7	29,800
527	1170	231	-9.2	119,600
528	1502	542	-4.6	53,400
530	1728	620	-2.0	48,000
532	507	1011	-27.4	30,000
533	870	489	-14.7	57,900
534	1347	1085	-6.9	27,300
535	1513	346	-4.5	77,800
536	308	654	<-35.0	46,000
538	1851	689	-0.7	44,100
539	1463	982	-5.1	31,100
540	909	561	-13.9	52,000
541	625	289	-21.7	93,100
542	1164	198	-9.2	146,200
543	803	655	-16.2	45,900
544	1259	1143	-8.0	25,200
545	856	1526	-15.0	12,200
546	803	1071	-16.2	27,800
547	1162	274	-9.3	98,400
548	128	1321	<-35.0	19,000
549	1355	1122	-6.8	25,900
550	595	866	-23.0	35,800
552	1369	494	-6.6	57,500
553	992	405	-12.2	67,600
555	1125	410	-9.8	66,900
556	705	975	-18.9	31,400
557	1477	1030	-4.9	29,300
558	980	583	-12.5	50,400
559	700	1109	-19.1	26,400
560	1028	621	-11.5	48,000
562	898	794	-14.1	38,900
564	789	1446	-16.6	14,900
565	777	766	-16.9	40,200
566	980	328	-12.5	81,900
567	1519	611	-4.4	48,600
569	1212	661	-8.6	45,600
570	760	594	-17.4	49,700
571	618	956	-21.9	32,100
573	1142	771	-9.6	40,000
574	532	787	-26.2	39,300
575	771	250	-17.1	109,200
576	1068	534	-10.8	54,100
577	822	734	-15.7	41,800
578	914	754	-13.8	40,800
579	1064	794	-10.8	38,900
580	1524	714	-4.4	42,800
581	1392	783	-6.3	39,400
582	982	686	-12.4	44,200
584	1487	672	-4.8	45,000
585	758	731	-17.4	41,900
586	687	1152	-19.5	24,900
587	930	523	-13.5	55,000
588	1888	774	-0.4	39,900
589	642	485	-21.1	58,300
590	1317	519	-7.3	55,300
591	65	1548	<-35.0	11,500
592	1014	614	-11.7	48,400
593	732	176	-18.1	172,300
594	1627	478	-3.0	59,000
595	1009	1426	-11.8	15.500
596	619	269	-21.9	100,500
597	1176	461	-9.1	60,700
598	1465	1044	-5.0	28,800
599	741	1188	-17.9	23,600
600	907	402	-14.0	68,000
601	687	658	-19.5	45,800
602	712	1138	-18.7	25,400
603	898	181	-14.1	165,200
604	783	1461	-16.7	14,400
605	736	223	-18.0	125,300
606	629	273	-21.6	98,700
607	1064	286	-10.8	94,000
608	883	503	-14.5	56,700
609	2012	610	>0.0	48,700
610	1255	903	-8.1	34,200
612	1103	391	-10.1	69,600
613	778	265	-16.9	102,000
614	824	518	-15.7	55,400
615	1095	195	-10.3	149,100
616	1759	478	-1.6	59,000
617	994	372	-12.1	72,900
618	751	374	-17.6	72,400
619	1429	518	-5.7	55,300
620	1050	520	-11.1	55,200
621	923	1105	-13.7	26,600
622	1462	622	-5.1	47,900
623	759	225	-17.4	124,000
624	758	1038	-17.4	29,000
625	1438	606	-5.5	48,900
626	1096	1089	-10.2	27,200
627	942	548	-13.3	53,000
628	809	621	-16.0	48,000
629	899	979	-14.1	31,300
630	1135	1321	-9.6	19,100
631	979	615	-12.5	48,300
632	1542	1076	-4.1	27,600
633	1345	814	-6.9	38,000
634	409	950	-32.2	32,400
635	1165	704	-9.2	43,300
636	774	604	-17.0	49,000
637	1263	524	-8.0	54,800
638	952	411	-13.1	66,700
639	1717	575	-2.1	51,000
640	994	292	-12.1	92,000
641	165	1224	<-35.0	22,400
642	803	251	-16.2	108,900
643	719	296	-18.5	90,700
644	1100	294	-10.2	91,400
645	534	1263	-26.1	21,000
646	1153	1038	-9.4	29,000
648	1246	204	-8.2	140,000
649	14	1406	<-35.0	16,200
650	1713	1049	-2.1	28,600
651	1986	1183	>0.0	23,800
652	1378	816	-6.5	38,000
653	1442	1165	-5.5	24,400
654	650	806	-20.8	38,400
655	1111	551	-10.0	52,700
656	1095	861	-10.3	36,000
657	1524	540	-4.4	53,600
658	1777	860	-1.4	36,000
659	391	584	-33.4	50,400
660	977	565	-12.5	51,700
661	658	166	-20.5	187,500
662	732	312	-18.1	86,100
663	1787	567	-1.2	51,500
664	888	268	-14.4	100,900
665	889	775	-14.3	39,800
666	715	221	-18.6	126,300
667	781	227	-16.8	122,400
668	646	165	-21.0	189,100
669	1116	353	-9.9	76,300
670	1382	643	-6.4	46,600
671	547	789	-25.3	39,200
673	984	746	-12.4	41.200
674	1661	448	-2.7	62,100
675	1523	562	-4.4	51,900
676	708	642	-18.8	46,700
677	919	615	-13.7	48,300
678	1085	551	-10.5	52,700
679	600	923	-22.7	33,400
680	1237	1004	-8.3	30,300
681	1103	283	-10.1	95,100
682	1406	477	-6.1	59,100
683	1596	249	-3.4	109,800
684	555	699	-24.8	43,500
685	1167	1313	-9.2	19,300
686	1932	790	0.0	39,100
687	1545	619	-4.1	48,100
688	1456	764	-5.2	40,300
689	1011	953	-11.8	32,300
690	1995	270	>0.0	100,200
691	812	888	-16.0	34,900
692	1154	1461	-9.4	14,400
693	1993	819	>0.0	37,800
694	1628	656	-3.0	45,900
695	928	254	-13.6	107,000
696	1854	715	-0.6	42,700
697	1997	345	>0.0	78,000
698	957	563	-13.0	51,800
699	1540	730	-4.2	42,000
702	577	900	-23.8	34,400
703	1610	562	-3.2	51,900
705	1278	571	-7.8	51,200
706	1841	704	-0.7	43,300
707	1018	1386	-11.7	16,900
709	1074	1145	-10.7	25,100
710	293	889	<-35.0	34,800
712	720	412	-18.5	66,600
713	1386	841	-6.4	36,800
714	1328	263	-7.1	103,100
715	698	433	-19.1	63,900
716	701	481	-19.0	58,700
717	1875	699	-0.5	43,600
718	575	702	-23.9	43,400
719	1216	204	-8.6	140,400
721	1069	464	-10.8	60,400
722	1272	506	-7.9	56,400
723	958	822	-13.0	37,700
724	763	395	-17.3	69,100
725	720	916	-18.5	33,700
726	1476	415	-4.9	66,200
727	1846	473	-0.7	59,400
728	510	783	-27.3	39,400
729	1217	1126	-8.6	25,800
730	1858	724	-0.6	42,300
731	665	765	-20.2	40,300
733	1321	312	-7.2	85,900
734	719	427	-18.5	64,600
735	1101	473	-10.2	59,500
736	1359	569	-6.7	51,400
738	696	220	-19.2	127,600
739	687	409	-19.5	67,000
740	1205	256	-8.7	106,200
741	995	563	-12.1	51,900
742	898	596	-14.1	49,500
743	881	181	-14.5	165,900
744	1951	686	>0.0	44,200
745	726	168	-18.3	183,600
746	999	643	-12.0	46,600
748	182	1503	<-35.0	13,000
749	2005	649	>0.0	46,300
750	1448	575	-5.4	51,000
751	792	266	-16.5	101,900
752	469	296	-28.9	90,600
754	664	254	-20.3	107,000
755	1195	184	-8.8	161,000
756	1821	1113	-0.9	26,300
757	909	246	-13.9	111,000
760	790	133	-16.5	264,900

MSN	X	Y	CPKpI	SDSMW
761	1398	733	-6.2	41,800
763	1416	1085	-5.9	27,300
764	2020	569	>0.0	51,400
765	651	475	-20.8	59,300
766	1052	1149	-11.1	25,000
767	1968	468	>0.0	59,900
768	1330	685	-7.1	44,300
769	1970	613	>0.0	48,500
770	857	617	-15.0	48,200
771	1337	974	-7.0	31,500
773	1576	502	-3.7	56,700
775	969	824	-12.8	37,600
776	1438	708	-5.5	43,100
777	1539	458	-4.2	61,000
778	850	434	-15.1	63,800
779	700	411	-19.1	66,800
780	1052	1136	-11.1	25,500
784	1413	529	-6.0	54,400
785	1364	885	-6.7	35,000
786	1822	835	-0.9	37,100
787	893	392	-14.3	69,500
790	616	882	-22.0	35,100
791	451	1429	-29.8	15,400
792	777	377	-16.9	72,000
793	1536	1543	-4.2	11,700
794	1461	807	-5.1	38,300
796	388	546	-33.6	53,100
797	1126	212	-9.8	133,700
798	933	437	-13.5	63,400
799	1420	593	-5.9	49,800
800	1759	279	-1.6	96,500
801	624	865	-21.7	35,800
802	898	547	-14.2	53,000
803	1775	1468	-1.4	14,200
804	573	196	-24.0	148,400
805	203	494	<-35.0	57,400
806	980	1039	-12.5	29,000
807	902	308	-14.1	87,200
808	625	827	-21.7	37,500
809	1851	1015	-0.7	29,900
810	440	573	-30.9	51,100
811	1358	249	-6.8	109,700
812	851	393	-15.1	69,400
813	745	1246	-17.8	21,600
814	2028	810	>0.0	38,200
815	1086	645	-10.4	46,500
816	629	313	-21.6	85,700
817	1376	1177	-6.5	24,000
818	1771	790	-1.4	39,100
819	1045	263	-11.2	103,100
820	984	362	-12.4	74,600
821	1712	279	-2.2	96,700
822	1256	205	-8.1	139,200
823	1517	654	-4.4	46,000
824	1442	449	-5.5	62,000
825	1240	513	-8.3	55,800
826	1309	1014	-7.4	29,900
827	2012	708	>0.0	43,100
828	937	1405	-13.4	16,200
830	1342	756	-7.0	40,700
831	562	826	-24.5	37,500
832	1073	1039	-10.7	29,000
833	481	820	-28.5	37,800
834	501	581	-27.8	50,500
837	751	748	-17.6	41,100
838	635	833	-21.3	37,200
839	1494	459	-4.7	60,900
840	1952	301	>0.0	89,300
841	1585	1080	-3.6	27,500
842	571	1312	-24.1	19,400
843	1325	649	-7.2	46,300
844	1727	301	-2.0	89,200
845	630	679	-21.5	44,600
846	2016	905	>0.0	34,200
847	673	1200	-19.9	23,200
848	1863	271	-0.6	99,500
849	1166	523	-9.2	54,900
850	1535	1024	-4.2	29,600
851	1035	826	-11.4	37,500
852	834	542	-15.5	53,400
855	499	220	-27.8	127,100
856	1063	194	-10.9	150,500
857	887	890	-14.4	34,800
858	1448	639	-5.4	46,900
859	706	311	-18.9	86,200
860	1070	1066	-10.7	28,000
861	472	347	-28.8	77,600
862	674	480	-19.9	58,800
864	1307	499	-7.4	57,000
865	645	887	-21.0	34,900
866	827	1004	-15.6	30,300
868	685	494	-19.5	57,400
869	1807	402	-1.0	68,000
870	1323	783	-7.2	39,400
871	1228	1031	-8.4	29,300
872	1904	346	-0.3	77,700
873	556	647	-24.8	46,400
874	1540	756	-4.2	40,700
875	1566	777	-3.8	39,700
876	1198	351	-8.8	76,800
877	1076	720	-10.6	42,500
878	1161	1111	-9.3	26,400
879	647	757	-20.9	40,700
880	1756	594	-1.6	49,700
881	1543	278	-4.1	97,100
883	1432	890	-5.7	34,800
884	922	689	-13.7	44,100
885	1103	414	-10.1	66,400
886	1501	607	-4.6	48,900
887	798	1103	-16.3	26,600
888	636	634	-21.3	47,200
889	951	759	-13.1	40,600
890	717	548	-18.6	52,900
891	1123	229	-9.8	121,200
892	891	413	-14.3	66,400
894	1245	234	-8.2	117,800
895	1962	346	>0.0	77,700
896	1322	626	-7.2	47,700
897	420	570	-31.4	51,300
898	662	428	-20.3	64,500
899	845	243	-15.3	113,000
900	624	703	-21.7	43,400
901	931	1094	-13.5	27,000
903	799	229	-16.3	121,000
904	765	520	-17.2	55,200
905	775	889	-17.0	34,800
907	888	824	-14.4	37,600
908	828	1303	-15.6	19,700
910	681	1544	-19.7	11,700
911	1544	301	-4.1	89,100
913	1606	387	-3.3	70,400
914	1237	688	-8.3	44,100
916	1442	749	-5.5	41,100
917	1260	367	-8.0	73,700
919	764	1541	-17.3	11,700
920	1133	1123	-9.7	25,900
921	1123	380	-9.8	71,500
923	829	242	-15.6	113,200
924	1131	318	-9.7	84,300
925	1441	874	-5.5	35,400
926	679	219	-19.7	128,200
927	1487	1191	-4.8	23,500
928	1082	775	-10.5	39,800
929	1231	816	-8.4	38,000
931	1609	670	-3.3	45,100
932	810	900	-16.0	34,400
933	965	520	-12.8	55,100
934	947	462	-13.2	60,600
936	865	843	-14.8	36,800
937	1421	1056	-5.9	28,400
939	1197	827	-8.8	37,500
941	1765	885	-1.5	35,000
942	602	472	-22.7	59,600
943	312	498	<-35.0	57,100
944	993	491	-12.1	57,700
945	1300	269	-7.5	100,300
946	630	423	-21.6	65,100
947	187	736	<-35.0	41,600
948	1380	344	-6.5	78,200
949	1766	665	-1.5	45,400
950	1038	193	-11.3	151,000
951	860	152	-14.9	213,000
952	957	701	-13.0	43,400
954	503	547	-27.6	53,000
955	1938	712	>0.0	42,900
957	1010	816	-11.8	37,900
959	768	174	-17.2	174,900
960	596	419	-23.0	65,700
961	557	409	-24.8	67,100
962	887	320	-14.4	83,900
963	564	334	-24.5	80,500
964	969	1155	-12.8	24,800
965	671	255	-20.0	106,600
966	1204	798	-8.7	38,700
967	910	154	-13.9	210,300
968	609	1048	-22.3	28,700
969	1285	206	-7.7	138,900
970	822	232	-15.8	119,300
971	976	437	-12.6	63,400
972	403	567	-32.6	51,600
974	279	495	<-35.0	57,400
975	844	981	-15.3	31,200
976	1124	295	-9.8	91,100
977	994	664	-12.1	45,400
978	1612	642	-3.2	46,700
979	749	1141	-17.7	25,300
980	1064	642	-10.8	46,700
981	1197	911	-8.8	33,900
983	1762	1508	-1.6	12,800
984	1344	317	-6.9	84,700
985	1024	1105	-11.5	26,600
987	739	1159	-17.9	24,600
988	816	555	-15.9	52,400
990	785	361	-16.7	74,900
991	1159	317	-9.3	84,500
992	1090	928	-10.4	33,300
993	1030	701	-11.5	43,400
994	847	811	-15.2	38,200
995	902	461	-14.1	60,700
996	888	847	-14.4	36,600
997	1815	579	-0.9	50,700
998	1205	504	-8.7	56,500
999	617	289	-22.0	93,100
1000	968	290	-12.8	92,700
1001	970	771	-12.7	40,000
1002	1736	478	-1.9	58,900
1003	643	1184	-21.1	23,700
1006	822	487	-15.8	58,100
1007	875	279	-14.6	96,400
1009	291	644	<-35.0	46,600
1010	1386	745	-6.4	41,200
1011	459	541	-29.4	53,500
1012	679	661	-19.7	45,600
1013	1818	1128	-0.9	25,800
1014	1032	634	-11.4	47,200
1015	1629	994	-3.0	30,700
1016	1311	1134	-7.4	25,500
1017	1722	424	-2.0	65,000
1018	1015	743	-11.7	41,300
1020	1574	1219	-3.7	22,500
1021	781	484	-16.8	58,400
1022	1129	83	-9.7	591,300
1023	812	317	-15.9	84,600
1024	785	446	-16.7	62,400
1025	1290	739	-7.7	41,500

MSN	X	Y	CPKpI	SDSMW
1026	405	552	-32.5	52,600
1027	1298	848	-7.5	36,500
1028	856	547	-15.0	53,000
1030	1284	226	-7.7	123,200
1031	986	822	-12.3	37,700
1032	1547	403	-4.1	67,900
1033	1381	551	-6.4	52,700
1034	1525	496	-4.3	57,200
1035	1128	645	-9.7	46,500
1036	1226	274	-8.5	98,300
1039	1761	262	-1.6	103,600
1040	541	839	-25.7	36,900
1041	818	910	-15.8	34,000
1044	1036	485	-11.3	58,300
1045	1439	407	-5.5	67,300
1047	1540	250	-4.2	109,200
1048	1576	635	-3.7	47,100
1049	1089	411	-10.4	66,700
1050	949	1040	-13.2	28,900
1051	426	818	-31.1	37,800
1052	1583	1385	-3.6	16,900
1053	779	1092	-16.8	27,000
1054	1613	620	-3.2	48,000
1055	1380	377	-6.5	72,000
1056	284	663	<-35.0	45,500
1058	1261	746	-8.0	41,200
1060	393	605	-33.3	49,000
1061	1817	645	-0.9	46,600
1062	1245	746	-8.2	41,200
1064	1258	792	-8.1	39,000
1065	705	934	-18.9	33,000
1066	1181	734	-9.0	41,800
1067	529	658	-26.3	45,800
1068	508	696	-27.4	43,700
1069	1898	604	-0.3	49,100
1071	873	609	-14.7	48,700
1073	1768	1128	-1.5	25,800
1075	836	773	-15.4	39,900
1076	1863	861	-0.6	36,000
1078	826	566	-15.7	51,600
1081	971	483	-12.7	58,500
1083	1697	202	-2.3	142,300
1085	1157	794	-9.4	38,900
1090	620	910	-21.9	34,000
1092	1867	597	-0.5	49,500
1093	2019	894	>0.0	34,600
1094	1546	538	-4.1	53,700
1095	1545	477	-4.1	59,100
1098	61	935	<-35.0	33,000
1099	1954	237	>0.0	116,000
1101	588	1048	-23.3	28,600
1102	1050	667	-11.1	45,200
1103	457	797	-29.5	38,800
1105	1884	532	-0.4	54,200
1106	1714	649	-2.1	46,300
1107	1717	546	-2.1	53,100
1108	1976	722	>0.0	42,400
1111	547	1066	-25.3	28,000
1112	1348	621	-6.9	48,000
1115	1385	762	-6.4	40,400
1116	1078	816	-10.6	38,000
1117	975	787	-12.6	39,300
1118	1202	933	-8.7	33,100
1119	1022	1076	-11.6	27,600
1120	1905	616	-0.3	48,300
1121	1512	1301	-4.5	19,700
1122	1114	677	-9.9	44,700
1123	1464	452	-5.1	61,700
1125	1048	857	-11.1	36,200
1126	1122	802	-9.8	38,600
1128	1722	892	-2.1	34,700
1133	1098	825	-10.2	37,500
1139	1830	569	-0.8	51,400
1147	764	1182	-17.3	23,800
1148	1968	724	>0.0	42,300
1153	921	1158	-13.7	24,700
1154	1594	864	-3.5	35,900
1161	637	400	-21.3	68,400
1162	623	397	-21.8	68,800
1163	665	397	-20.2	68,700
1168	564	528	-24.4	54,500
1170	552	529	-25.0	54,500
1171	538	524	-25.9	54,800
1172	545	514	-25.5	55,700
1174	1099	522	-10.2	55,000
1176	1304	586	-7.5	50,200
1177	1366	539	-6.6	53,700
1178	1608	702	-3.3	43,400
1179	1485	224	-4.8	124,900
1180	1459	224	-5.2	124,900
1181	1431	223	-5.7	125,100
1182	1407	223	-6.1	125,200
1183	1383	224	-6.4	124,700
1184	1454	182	-5.3	164,400
1185	1422	183	-5.8	162,600
1186	1394	182	-6.3	164,300
1189	1171	214	-9.2	131,800
1190	1457	286	-5.2	94,200
1191	686	1114	-19.5	26,200
1192	265	893	<-35.0	34,700
1193	403	1292	-32.6	20,000
1194	344	1275	<-35.0	20,600
1195	505	1311	-27.6	19,400
1196	572	1293	-24.1	20,000
1197	639	1502	-21.2	13,000
1198	637	1402	-21.3	16,300
1199	614	1407	-22.1	16,200
1200	637	1431	-21.3	15,400
1201	1095	1394	-10.3	16,600
1202	1719	1545	-2.1	11,600
1203	791	668	-16.5	45,200
1204	964	1021	-12.9	29,700
1205	313	195	<-35.0	148,700
1208	306	194	<-35.0	149,800
1209	320	197	<-35.0	147,400
1210	326	197	<-35.0	146,600
1211	394	294	-33.2	91,400
1212	402	294	-32.7	91,200
1214	386	294	-33.7	91,400
1215	641	329	-21.2	81,600
1216	660	329	-20.4	81,600
1217	914	266	-13.8	101,800
1218	873	245	-14.7	112,000
1219	970	372	-12.7	72,900
1220	1021	298	-11.6	90,100
1221	1392	205	-6.3	139,500
1222	1354	203	-6.8	141,800
1223	1362	205	-6.7	139,500
1224	673	540	-19.9	53,600
1225	614	542	-22.1	53,400
1226	603	539	-22.6	53,600
1227	696	623	-19.2	47,800
1228	707	628	-18.9	47,500
1229	475	447	-28.7	62,300
1230	466	1282	-29.0	20,400
1231	759	1461	-17.4	14,400
1232	1324	1170	-7.2	24,200
1233	1583	1005	-3.6	30,300
1234	1865	809	-0.6	38,200
1235	1812	817	-1.0	37,900
1236	1411	703	-6.0	43,400
1237	1392	682	-6.3	44,500
1238	794	410	-16.4	66,900
1239	769	407	-17.1	67,300
1240	740	406	-17.9	67,500
1241	743	511	-17.8	55,900
1242	713	510	-18.7	56,000
1243	682	509	-19.6	56,100
1244	663	504	-20.3	56,500
1245	565	582	-24.4	50,500
1246	547	577	-25.3	50,800
1247	530	576	-26.3	50,900
1249	516	572	-27.0	51,200
1250	973	536	-12.7	53,900
1251	607	532	-22.4	54,200
1252	665	529	-20.2	54,400
1253	899	766	-14.1	40,200
1254	1311	746	-7.4	41,200
1255	1300	761	-7.5	40,400
1257	1938	712	0.0	42,900
1258	1806	718	-1.0	42,600
1259	1727	715	-2.0	42,700
1260	1629	713	-3.0	42,800
1261	1555	717	-4.0	42,600
1262	1468	717	-5.0	42,600
1263	1413	722	-6.0	42,400
1264	1340	717	-7.0	42,600
1265	1263	717	-8.0	42,600
1266	1182	720	-9.0	42,500
1267	1110	717	-10.0	42,600
1268	1055	717	-11.0	42,600
1269	999	717	-12.0	42,600
1270	959	715	-13.0	42,700
1271	905	712	-14.0	42,900
1272	857	714	-15.0	42,800
1273	810	705	-16.0	43,300
1274	774	711	-17.0	42,900
1277	737	708	-18.0	43,100
1278	702	711	-19.0	42,900
1279	671	710	-20.0	43,000
1280	645	710	-21.0	43,000
1281	617	707	-22.0	43,100
1282	595	704	-23.0	43,300
1283	573	700	-24.0	43,500
1284	552	695	-25.0	43,700
1285	536	694	-26.0	43,800
1286	515	687	-27.0	44,200
1287	496	683	-28.0	44,400
1288	467	669	-29.0	45,200
1289	447	667	-30.9	45,300
1290	427	655	-31.0	45,900
1291	412	655	-32.0	45,900
1292	397	652	-33.0	46,100
1293	381	654	-34.0	46,000
1294	365	653	-35.0	46,100
1295	348	653	<-35.0	46,100

Table 2. Table of some identified proteins

POP name	Protein name	MSN's	Basis for identification
IDS:3_ALPHA_HDDH	3-α-hydroxysteroid-dihydrodiol-dehydrogenase, an enzyme of steroid metabolism	137, 159	Pure protein and antibody provided by Dr. T.M. Penning, Department of Pharmacology, School of Medicine, University of Pennsylvania.
IDS:ACTIN_BETA	β cellular actin, a cytoskeletal protein	38	Homologous position with respect to other mammalian systems
IDS:ACTIN_GAMMA	γ cellular actin, a cytoskeletal protein	68	Homologous position with respect to other mammalian systems
IDS:ALBUMIN	Serum albumin, mature form.	21, 28, 33	Predominance in rat plasma
IDS:APO_A-I	Apo A-I plasma lipoprotein, mature form (tentative).	236, 463	Presence in rat plasma, regulation by some lipid-lowering drugs
IDS:CALMODULIN	Calmodulin, an acidic cytosolic calcium-binding protein	123, 649	Homologous position with respect to other mammalian systems
IDS:CATALASE	Catalase (peroxisomal)	54, 61, 106	Presence in purified peroxisomes, similarity in position to mouse catalase
IDS:CPKSPOTS	Spots contributed by the CPK charge standards (not rat liver proteins)	1257 - 1295	
IDS:CPS	Carbamoyl phosphate synthase	114, 157, 167, 174, 1184, 1185, 1186, 1222	Pure protein provided by Dr. Margaret Marshall, Department of Pharmacology, Medical School, University of Wisconsin - Madison.
IDS:CYTOCHROME_B5	Cytochrome b5	87, 477	Pure protein provided by Dr. Andrew Parkinson, Department of Pharmacology, Toxicology and Therapeutics, University of Kansas Medical Center
IDS:FABP-L	Liver fatty-acid binding protein	227	Pure protein provided by Dr. Nathan Bass, Department of Medicine, University of California School of Medicine, San Francisco
IDS:HMG-COA_SYNTHASE	Cytosolic HMG-CoA Synthase	133, 144, 235, 413	Antibody provided by Dr. Michael Greenspan, Merck Sharp & Dohme Research Laboratories, Rahway, NJ
IDS:LAMIN_B	Lamin B, a nuclear protein	415, 734	Homologous position with respect to other mammalian systems
IDS:MITCON:1	Mitcon:1 (F1 ATPase β subunit), a mitochondrial inner membrane	17, 49, 71, 340, 1245, 1246, 1247, 1249	Homologous position with respect to other mammalian systems, presence in mitochondria
IDS:MITCON:2	Mitcon:2, a mitochondrial matrix stress protein equivalent to E.	15, 25, 110, 1241, 1242, 1243, 1244	Homologous position with respect to other mammalian systems, presence in mitochondria
IDS:MITCON:3	Mitcon:3, a mitochondrial matrix stress protein, likely analog of	18, 35, 226, 600, 1238, 1239, 1240	Homologous position with respect to other mammalian systems, presence in mitochondria
IDS:NADPH_P450_RED	NADPH cytochrome P-450 reductase, frequently co-induced with P-450's	175, 251, 812	Pure protein provided by Dr. Andrew Parkinson, Department of Pharmacology, Toxicology and Therapeutics, University of Kansas Medical Center
IDS:PDI	Protein disulphide isomerase 1	168, 1170, 1171, 1172	Sequence information obtained by R.M. Van Frank, Lilly Research Laboratories, Indianapolis
IDS:PLASMA_PROTEINS	Rat plasma proteins observed in liver	21, 28, 33, 44, 72, 102, 115, 197, 236, 246, 248, 257, 293, 332, 347, 364, 369, 419, 432, 463, 468, 518, 562, 605, 623, 666, 667, 725, 738, 790, 865, 903, 926	Plasma coelectrophoresis studies
IDS:PRO-ALBUMIN	Serum albumin precursor	47, 93	Relative position to mature albumin, presence in microsomes
IDS:PYRCARBOX	Pyruvate carboxylase	179, 1180, 1181, 1182, 1183	Pavlica, R.J., et al., BBA (1990) *1022* 115-125.
IDS:SOD	Superoxide dismutase	135	Sequence information obtained by R.M. Van Frank, Lilly Research Laboratories, Indianapolis
IDS:TUBULIN_ALPHA	α tubulin, a cytoskeletal protein	56, 132, 1224, 1252	Homologous position with respect to other mammalian systems
IDS:TUBULIN_BETA	β tubulin, a cytoskeletal protein	50, 1225, 1226, 1251	Homologous position with respect to other mammalian systems

Table 3. Computed p*I*'s of two sets of carbamylated protein standards: Rabbit muscle CPK and human hemoglobin (Hb)

	Protein Name	PIR Name	#ASP 3.9	#GLU 4.1	#HIS 6.0	#LYS 10.8	#ARG 12.5	NH2- 7.0	Calc pI	Real CPK
0	Rabbit muscle CPK	KIRBCM	28	27	17	34	18	1	6.84	0.0
-1			28	27	17	33	18	1	6.67	-1
-2			28	27	17	32	18	1	6.54	-2
-3			28	27	17	31	18	1	6.42	-3
-4			28	27	17	30	18	1	6.31	-4
-5			28	27	17	29	18	1	6.21	-5
-6			28	27	17	28	18	1	6.12	-6
-7			28	27	17	27	18	1	6.03	-7
-8			28	27	17	26	18	1	5.94	-8
-9			28	27	17	25	18	1	5.85	-9
-10			28	27	17	24	18	1	5.76	-10
-11			28	27	17	23	18	1	5.67	-11
-12			28	27	17	22	18	1	5.58	-12
-13			28	27	17	21	18	1	5.48	-13
-14			28	27	17	20	18	1	5.39	-14
-15			28	27	17	19	18	1	5.29	-15
-16			28	27	17	18	18	1	5.20	-16
-17			28	27	17	17	18	1	5.12	-17
-18			28	27	17	16	18	1	5.04	-18
-19			28	27	17	15	18	1	4.96	-19
-20			28	27	17	14	18	1	4.89	-20
-21			28	27	17	13	18	1	4.83	-21
-22			28	27	17	12	18	1	4.77	-22
-23			28	27	17	11	18	1	4.71	-23
-24			28	27	17	10	18	1	4.66	-24
-25			28	27	17	9	18	1	4.61	-25
-26			28	27	17	8	18	1	4.56	-26
-27			28	27	17	7	18	1	4.52	-27
-28			28	27	17	6	18	1	4.48	-28
-29			28	27	17	5	18	1	4.44	-29
-30			28	27	17	4	18	1	4.40	-30
-31			28	27	17	3	18	1	4.36	-31
-32			28	27	17	2	18	1	4.32	-32
-33			28	27	17	1	18	1	4.29	-33
-34			28	27	17	0	18	1	4.25	-34
-35			28	27	17	0	18	0	4.22	-35
0	Hb-beta, human	HBHU	7	8	9	11	3	1	7.18	
-1			7	8	9	10	3	1	6.79	
-2			7	8	9	9	3	1	6.53	-1.8
-3			7	8	9	8	3	1	6.32	-3.2
-4			7	8	9	7	3	1	6.13	-5.3
-5			7	8	9	6	3	1	5.96	-7.2
-6			7	8	9	5	3	1	5.78	-10.0
-7			7	8	9	4	3	1	5.59	-12.3
-8			7	8	9	3	3	1	5.37	-15.5
-9			7	8	9	2	3	1	5.14	-18.0
-10			7	8	9	1	3	1	4.91	-21.0
-11			7	8	9	0	3	1	4.71	-25.5
-12			7	8	9	0	3	0	4.54	-27.2

Table 4. Computed p*I*'s of some known proteins related to measured CPK p*I*'s

	Protein Name	PIR Name	#ASP 3.9	#GLU 4.1	#HIS 6.0	#LYS 10.8	#ARG 12.5	Calc pI	Real CPK
0	Creatine phospho kinase (CPK), rabbit muscle	KIRBCM	28	27	17	34	18	6.84	0.0
1	Fatty acid-binding protein, rat hepatic	FZRTL	5	13	2	16	2	7.83	-3.0
2	b2-microglobulin, human	MGHUB2	7	8	4	8	5	6.09	-5.0
3	Carbamoyl-phosphate synthase, rat	SYRTCA	72	96	28	95	56	5.97	-5.5
4	Proalbumin (serum albumin precursor), rat	ABRTS	32	57	15	53	27	5.98	-6.2
5	Serum albumin, rat	ABRTS	32	57	15	53	24	5.71	-9.0
6	Superoxid dismutase (Cu-Zn, SOD), rat	A26810	8	11	10	9	4	5.91	-9.2
7	Phospholipase C, phophoinositide-specific (?), rat	A28807	34	42	9	49	21	5.92	-9.2
8	Albumin, human	ABHUS	36	61	16	60	24	5.70	-11.9
9	Apo A-I lipoprotein, rat	A24700	18	24	6	23	12	5.32	-13.7
10	proApo A-I lipoprotein, human	LPHUA1	16	30	6	21	17	5.35	-14.3
11	NADPH cytochrome P-450 reductase, rat	RDRTO4	41	60	21	38	36	5.07	-15.6
12	Retinol binding protein, human	VAHU	18	10	2	10	14	5.04	-16.9
13	Actin beta, rat	ATRTC	23	26	9	19	18	5.06	-17.2
14	Actin gamma, rat	ATRTC	20	29	9	19	18	5.07	-16.8
15	Apo A-I lipoprotein, human	LPHUA1	16	30	5	21	16	5.10	-17.5
16	Apo A-IV lipoprotein, human	LPHUA4	20	49	8	28	24	4.88	-19.7
17	Tubulin alpha, rat	UBRTA	27	37	13	19	21	4.66	-19.8
18	F1ATPase beta, bovine	PWBOB	25	36	9	22	22	4.80	-21.0
19	Tubulin beta, pig	UBPGB	26	36	10	15	22	4.49	-22.5
20	Protein disulphide isomerase (PDI), rat hepatic	ISRTSS	43	51	11	51	9	4.07	-25.0
21	Cytochrome b5, rat	CBRT5	10	15	6	10	4	4.59	-26.0
22	Apo C-II lipoprotein, human	LPHUC2	4	7	0	6	1	4.44	-30.5
	Amino acid pI assumed in calulation:		3.9	4.1	6.0	10.8	12.5		

ELECTROPHORESIS
An International Journal
11'91

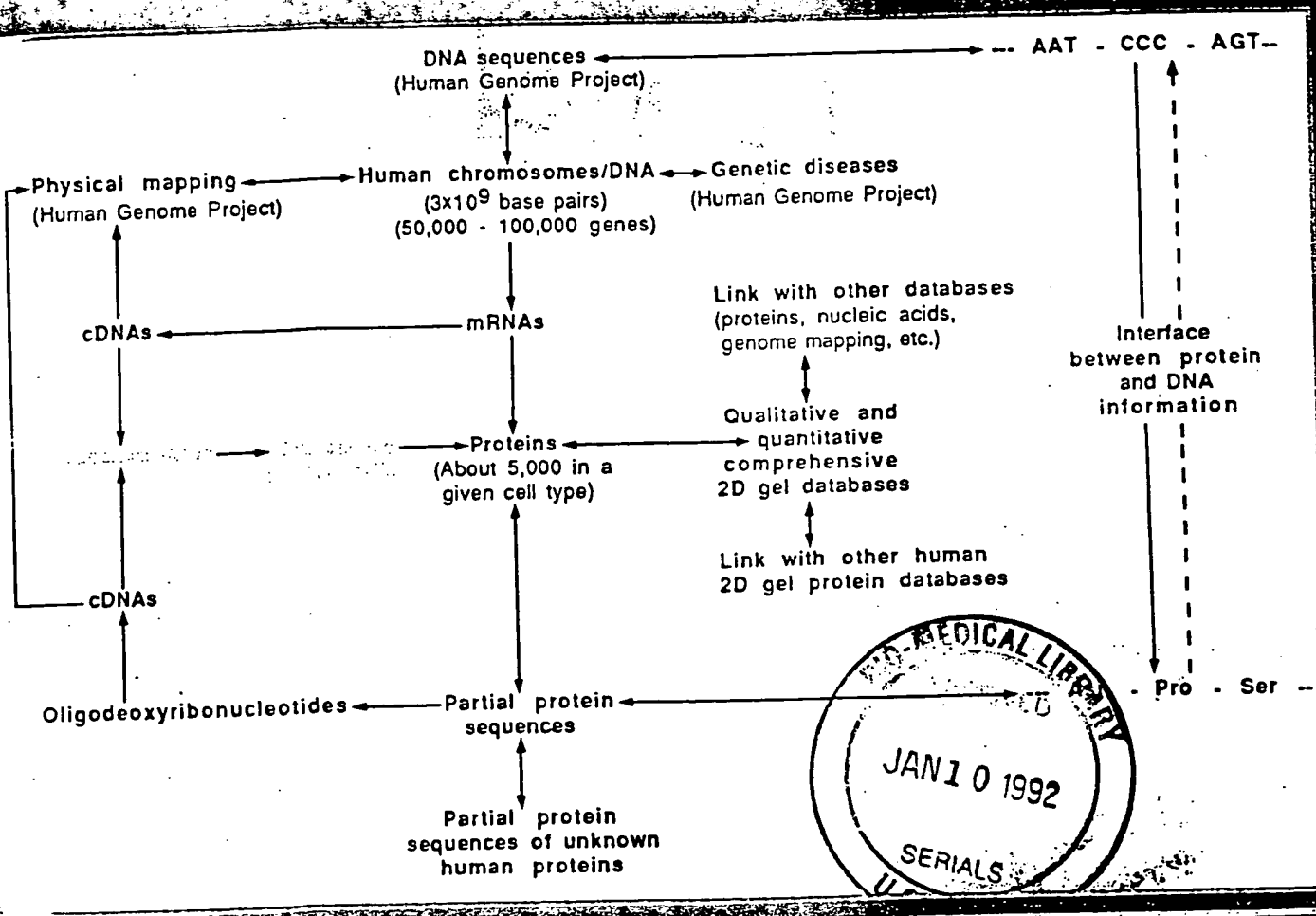

TWO-DIMENSIONAL GEL PROTEIN DATABASES

Editor: J. E. Celis

VCH

ELECTROPHORESIS

An International Journal

Indexed in: BIOSIS, Current Contents, MEDLARS
ISSN 0173-0835
ELCTDN 12 (11) 763–996 (1991)

TWO-DIMENSIONAL GEL PROTEIN DATABASES
Editor: J. E. Celis

Editorial